Reliability-Based Optimization of Rail Inspection

by

Takashi Kashima

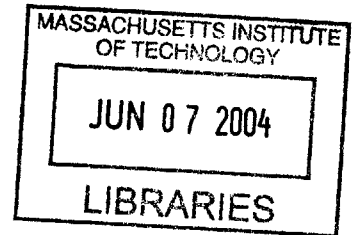M. Eng., Architecture and Civil Engineering
Kobe University, 1997

Submitted to the Department of Civil and Environmental Engineering
in partial fulfillment of the requirements for the degree of
Master of Science in Civil and Environmental Engineering

at the

Massachusetts Institute of Technology

June 2004

Signature of Author.......

Department of Civil and Environmental Engineering
May 7, 2004

Certified by..........................

Jerome J. Connor
Professor of Civil and Environmental Engineering
Thesis Supervisor

Accepted by................

Heidi M. Nepf
Chairman, Department Committee on Graduate Students

Reliability-Based Optimization of Rail Inspection

by

Takashi Kashima

Submitted to the Department of Civil and Environmental Engineering
on May 7, 2004 in partial fulfillment of the
requirements for the degree of
Master of Science in Civil and Environmental Engineering

Abstract

This thesis proposes a quantitative method to optimize inspection/repair intervention in rail defect management. Rail defect management is important for track maintenance, since rails are the most significant and basic component of the track systems. Rail inspection is a fundamental intervention to prevent rail failure. Railroads have evolved the rail inspection interval based on their empirical judgement and on field data.

A crack size is predicted by linear elastic fracture mechanics (LEFM). The proposed method identifies the time-varying rail reliability due to deterioration, using data obtained from LEFM and from first-order reliability methods (FORM), which consider the uncertainty regarding the model. Since FORM is an approximation method, Monte Carlo simulation confirms the results.

To represent practical situations regarding rail defect management, an event tree (ET) analysis is performed. The ET is modeled to all events and actions with respect to inspection/repair intervention. The ET analysis evaluates the expected reliability of a rail after inspections and possible remedial actions. Based on these results, a life-cycle cost (LCC) model is formulated, taking into consideration the time value of money.

To this end, applications of the model to optimization of inspection intervals and to investigation of the effect of nondestructive testing and remedial actions on the LCC and the interval are analyzed. As a result, it is possible to extend the present inspection interval. Additionally, the effect of detectability of nondestructive testing on the LCC is more significant than that of accuracy of nondestructive testing, and a proactive maintenance policy may reduce both the expected total cost and the number of inspections.

Thesis Supervisor: Jerome J. Connor
Title: Professor of Civil and Environmental Engineering

Acknowledgement

Contents

List of Figures

12

13

List of Tables

Chapter 1

Introduction

1.1 Overview

Railroad operation requires many employees due to the diverse and unique characteristics of railroad systems in comparison with other transportation industries. For instance, airline companies do not need to manage airports to operate their business even though they have many airplanes. Likewise, a bus business does not require managing and maintaining a highway to use it, though they have to pay for it. On the other hand, railroad firms generally have all the facilities such as tracks, rolling stock, stations, and electric lines, and have to work from planning, constructing, operating, and maintaining with respect to the railroad business.

Since track maintenance is among the most labor-intensive of company activities,

the reduction of maintenance is required for sound management of railroad companies. As a matter of fact, statistics show that rail maintenance cost is up to thirty percent of the total operation cost in East Japan Railway Company (JR East) as shown in Fig. 1.1. Given this huge investment, along with an increasing scarcity of resources as shown in Fig. 1.2, it is essential that the funds be used as efficiently as possible.

This thesis describes in depth optimization of rail inspection, which is a part of track maintenance management, based on the structural reliability theory taking into account the uncertainty of inspection equipment and of remedial actions. It proposes a method to determine the optimal number of rail inspections during the service life by minimizing the Life-Cycle Cost (LCC).

1.2 Motivation and Problem Statement

Rails deteriorate over time and need maintenance to detect and correct damage, deterioration, and cracks. Because rails are the most significant and basic component of railroad systems and the damaged rails may result in accidents, it is very important that rails should be maintained and inspected routinely. In other words, the reliability of rails depends upon the frequency and quality of the maintenance programs. In spite of the fact that railroad companies have attempted to reduce the number of broken rails by making use of various management techniques, the numbers have not yet reached zero. Fig. 1.3

shows the number of broken rails during the fiscal year from 1999 to 2001 in JR East, and Fig. 1.4 depicts the location of the defects in the broken rails. The railroad industry still has a hurdle to overcome this issues regarding track maintenance. Further, optimization of rail maintenance has the potential for significant industry-wide benefits.

In order to prevent rails from breaking during the service life, railroad companies have two policy options in rail defect management: one is to improve the material, making it more durable; the other is to increase the frequency of rail inspection. Yet it is a difficult task to develop a new material that will not develop cracks during its service life. As for the frequency of rail inspection, it is also expensive for the company to significantly increase the frequency of rail inspection. Neither option is a practical solution to the problem of rail failure.

An efficient rail maintenance program requires careful planning based on potential modes of the rail failure, the history of repairs done, and the frequency and intensity of applied trainload. Effective maintenance/repair intervention can enhance the reliability of railroad systems, and, at the same time, maintain a reliability level that reduces the possibility of costly failures in the future. Optimization of rail inspections based on a probabilistic model can reduce rail maintenance work and its cost. Working out a better strategy for rail inspection will allow railroad companies to save maintenance costs without increased risk to passengers.

The Japanese government requires railroad companies to make company regulations for maintaining tracks. Each railroad company is able to institute specific inspection and repair regulations in detail, such as the frequency of inspection, the

method of inspection, and the criterion of judgment, as long as the rules are consistent with the government codes. Regarding remedial actions accompanied with rail inspections, JR East establishes the rules shown in Table1.1. Table 1.2 shows the rules ratified by the Department of Transportation (DOT) for reference. JR East institutes the rail inspection rules for each unit rail, basically 25 [m]. JR East has a database that has the age and accumulation of the trainload for the maintenance management. JR East can identify the location of the rails and the results of rail inspections by using the database.

JR East set up rules by which the track engineers have to replace the rails at 400 Million Gross Tons (MGT) with new one. This value is derived from Miner's damage accumulation law and empirical judgement. In general, either Miner's law or particular probability distributions such as Weibull and Exponential distribution that are a part of extreme distributions are used to evaluate fatigue life and reliability in steel materials such as rails. However, this probabilistic model has some drawbacks that make it unfriendly to use in the reliability analysis other than estimation of its life expectancy. One reason is that it is difficult to determine its shape parameter to represent rail characteristics, even though Bayes' Theorem is used as the epistemic model. The other is that it is difficult for the Weibull model to reflect the inspection results, since the Weibull model does not include information about the crack size. In contrast, the railroad companies obtain the results of inspection from crack size information.

Therefore, it is essential for railroad companies to establish a quantitative method for optimization of rail inspection/repair intervention, taking into consideration on capability and quality of inspection and repair policy.
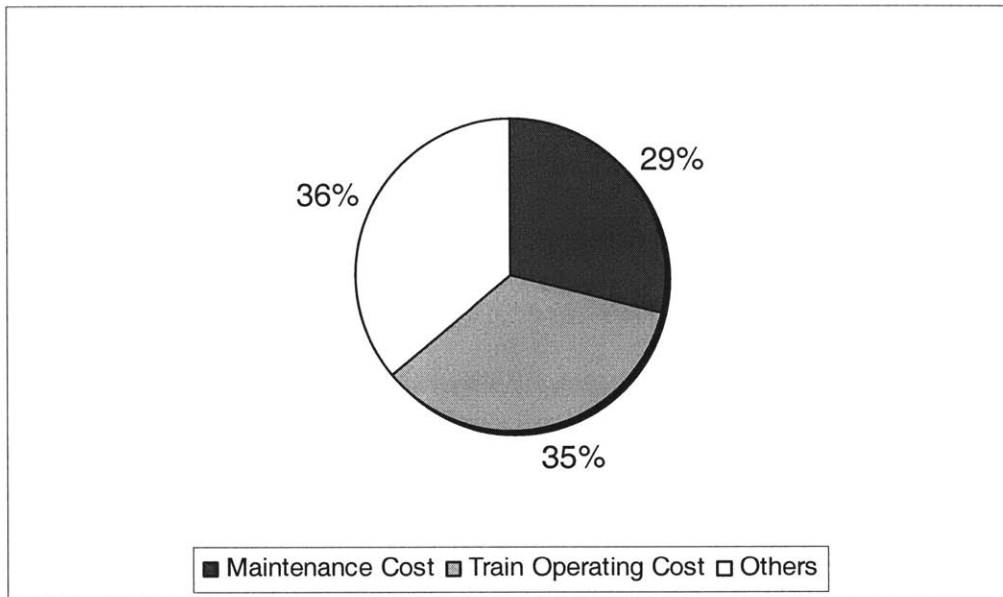
Fig. 1.1 Operating Cost in Railroad Business of JR East
Inazu, H. (2003), "Innovation of Maintenance," JR East Technical Review, No2, pp. 4-5.
http://www.jreast.co.jp/development/english/paper/contents02.html
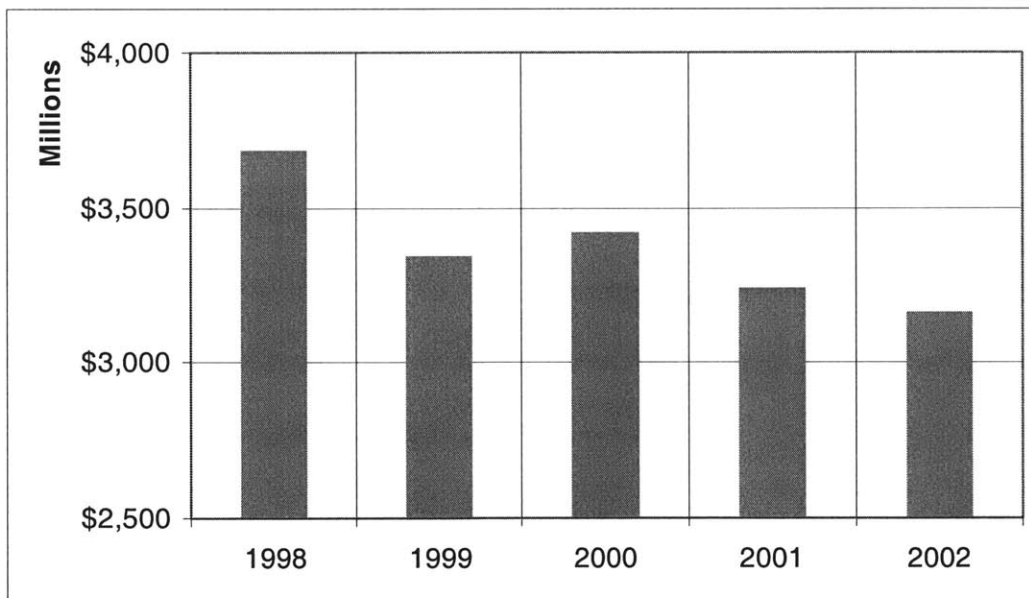
Fig. 1.2 Operating Income in JR East
JR East (2002), "Annual Report," pp. 44-45. (1dollar=100 yen)
http://www.jreast.co.jp/e/investor/finance/ar2002.html
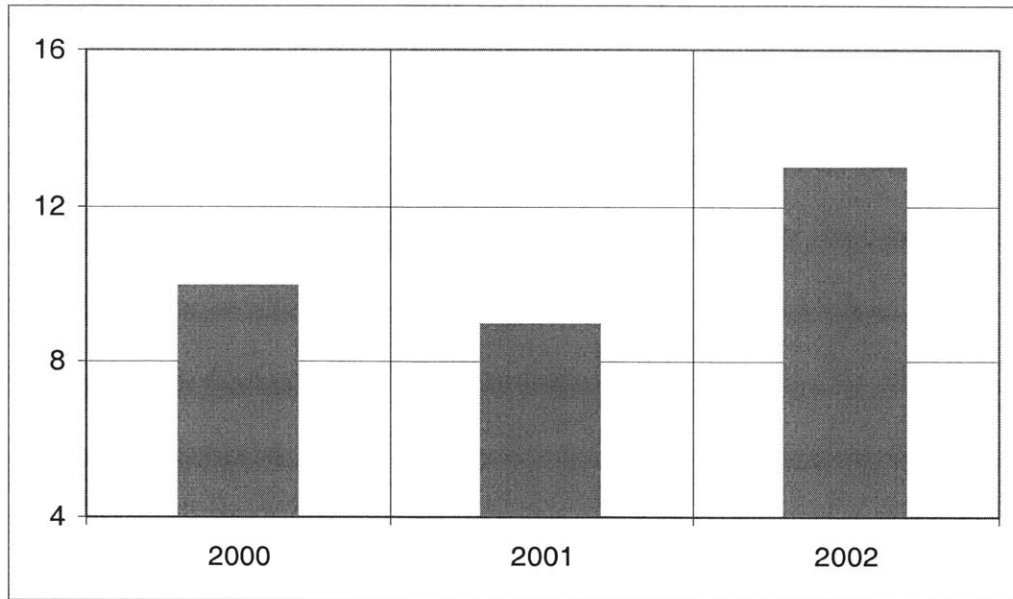
Fig. 1.3 The Number of Broken Rails in JR East
Ohsawa, S. (2003), "JR Higashi-Nihon ni okeru re-ru sessonn taisaku," Nippon Tetsudou Shisetsu Kyokai, Nippon Tetsudou Shisetsu Kyokai-Shi, April, pp. 265-268.
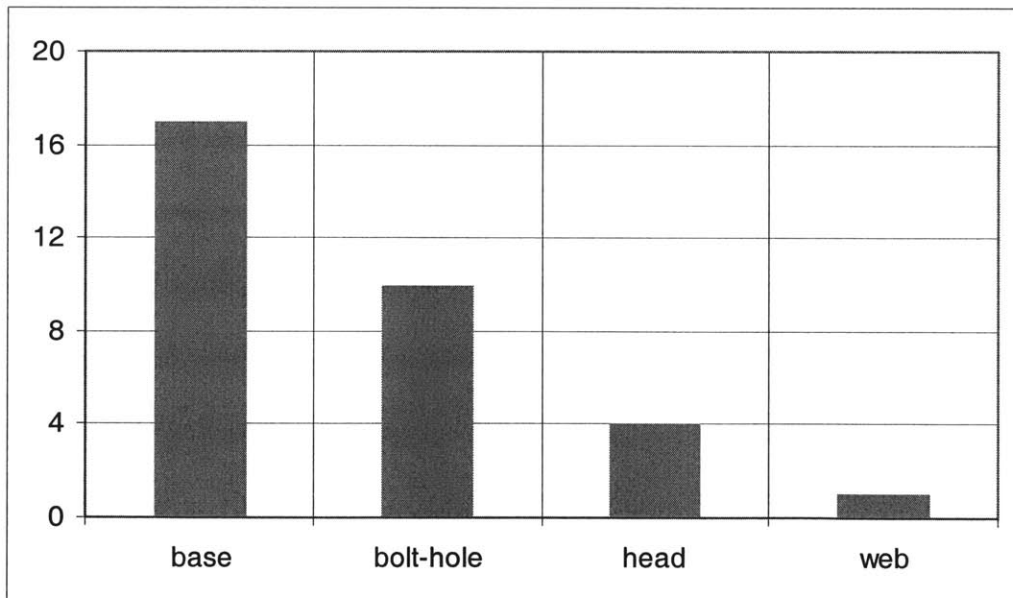
Fig. 1.4 The Location of Defects in Broken Rails in JR East
Ohsawa, S. (2003),"JR Higashi-Nihon ni okeru re-ru sessonn taisaku," Nippon Tetsudou Shisetsu Kyokai, Nippon Tetsudou Shisetsu Kyokai-Shi, pp. 265-268.

Table1.1 Remedial Action Table in JR East

Type of Defects	Criteria [mm]	Remedial action
Vertical split head	$5 \le a < 15$	Marking for check
	$15 \le a < 30$	Apply bolted joint bar and plan to replace
	$30 \le a$	Replace immediately
Split web	$2 \le a < 6$	Marking for check
	$6 \le a < 10$	Apply bolted joint bar and plan to replace
	$10 \le a$	Replace immediately
Broken Base	$a < 3$	Apply bolted joint bar and plan to replace
	$3 \le a$	Replace immediately
Bolt-hole crack	$a < 5$	Marking for check
	$5 \le a$	Replace immediately

JR East (2003), "Shisetsu-Kensetsu Hohki Ruisyu," pp. 327-328.

Table1.2 Remedial Action Table in DOT

Type of Defects	Criteria [mm]	Remedial action *if the rail is not replaced*
Vertical split head	$2.54 \le a < 5.08$	Limit operating speed over defective rail to 48 [km/h]
		Inspect the rail 30 days after it is determined to continue the track in use
Split web	$10.16 \le a$	Limit operating speed as authorized by track supervisor
		Operating speed cannot be over 48[km/h]
Broken Base	$2.54 \le a < 15.24$	Apply joint bars bolted within 10days after it is determined to continue the track in use
		After applying the joint bars, limit operating speed to 80[km/h]
Bolt-hole crack	$2.54 \le a < 3.81$	Limit operating speed over defective rail to 80 [km/h]
		Inspect the rail 30 days after it is determined to continue the track in use

Department of Transportation (1998), "Track Standards Part 213," pp. 33-41.

23

1.3 Objective

The main objective of this study is to develop a method for optimization of rail inspection/repair based on the structural reliability theory. The following are the sub-objectives to carry out the main purpose:

- Assessing crack growth during the service life while estimating the stress amplitude by variable trainloads.

- Evaluating the time-varying rail reliability profile, considering both rail inspections by Non-Destructive Testing (NDT) and remedial actions.

- Optimizing the number of rail inspections so as to minimize the expected total costs.

- Contemplating the specifications for the effect of changing NDT techniques and of remedial actions on the LCC and the optimal inspection interval.

1.4 Study Approach

Fig. 1.5 illustrates the structure of the study approach. Following literature reviews, a five-step analysis is used for optimization of rail inspections.

First of all, a literature review is performed to document the validation of the reliability-based approach for optimization of rail inspections. This review also identifies the way to formulate the reliability index of rails without using complex numerical

calculus, a formidable task. In addition to the review, another literature review regarding railroad maintenance is also carried out.

In a step-one analysis, Linear Elastic Fracture Mechanics (LEFM) based on Paris and Erdogan's kinetic crack growth law predicts the rail fatigue life using the results of stress amplitude estimates. The semi-elliptical crack model in LEFM shows the crack size of the rail base at arbitrary times. A continuously supported elastic model for railroad tracks is applied to determine the rail stress by a solving fourth-order differential equation based on engineering mechanics of rails. A superposition method calculates the total stress amplitude by combining each stress caused by a rolling stock axial load. For information about rail design parameters, general rails in conventional railroad systems in Japan are employed.

As a step-two analysis, First-Order Reliability Methods (FORM) create the reliability profile of rails as a reliability index: beta. The initial crack size, critical crack size, and material parameters are random variables in the analysis. It is noted that the variable stress amplitude converts to the effective stress range to characterize a stress spectrum. Moreover, the accuracy of the second-moment linear approximation is generally difficult to assess, because it will depend on the degree of non-linearity of the performance function in FORM. Therefore, a large sample Monte Carlo Simulation (MCS) verifies the reliability index calculated by FORM.

Third, an Event Tree (ET) analysis resolves all possible consequences of detecting defects and remedial actions with probability. Moreover, as a result of the ET analysis, the expected reliability index with time horizontal is calculated. Qualification and

accuracy of NDT are taken care of by use of a Probabilistic Density Function (PDF), and the PDF represents the uncertainty of remedial actions.

The fourth analysis of LCC optimizes the number of inspections so as to minimize the expected total cost, including the inspection cost, repair cost, and failure cost, considering the time value of money. When the frequency of inspections is high, the reliability is improved. However, the cost is also high. When the frequency of rail inspections is low, it is difficult to maintain operability. The most practical solution is to find an optimal number of inspections.

Finally, sensitivity analysis shows the effect of capability and precision of inspection device, repair regulation, and failure cost for the reliability of rail on the LCC and the frequency of inspections.
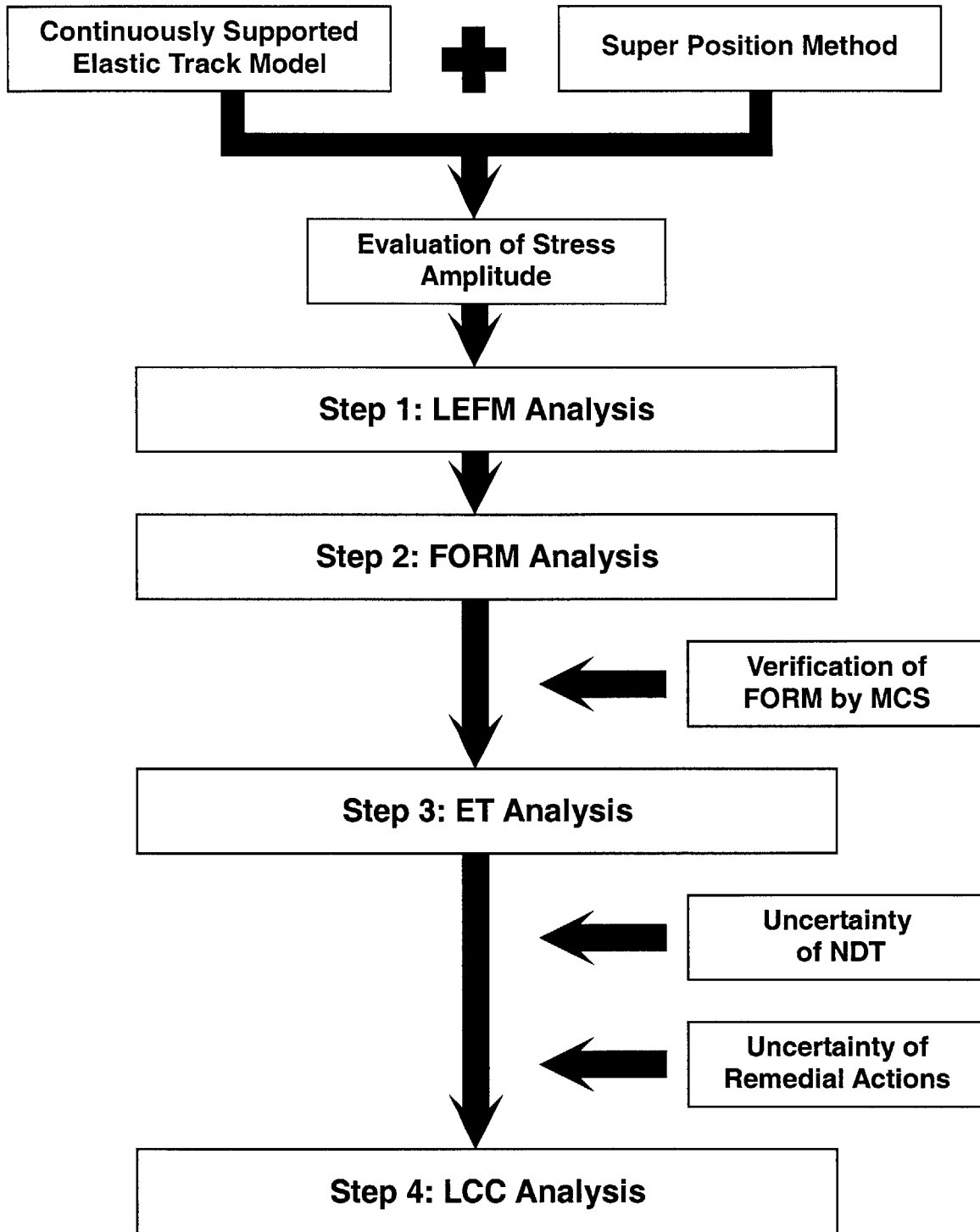
Fig. 1.5 Structure of Study Approach

1.5 Thesis Format

Fig. 1.6 shows the organization of this thesis. Following this introduction, the thesis consists of four remaining chapters.

Chapter 2 reviews the current literature on reliability-based optimization of inspection in both bridge structures and offshore structures. The efforts of the researchers to apply the structural reliability theory to making a decision about maintenance strategy are reviewed. In particular, the review is focused on different approaches to decide the optimal timing of inspection/repair and the characteristics of each structure. Moreover, this chapter presents literature review regarding railroad maintenance for rail car trucks as well as rail fatigue analysis.

Chapter 3 lays out the research methodology for this thesis. It demonstrates how crack size grows and how FORM accommodates uncertainty and calculates a reliability index by using random variable data. The method generates a time-varying reliability index of rails.

Chapter 4 gives the optimal number of inspections and demonstrates sensitivity analysis as a part of applications of a method developed during this study. Through the sensitivity analysis, the effect of quality of inspection is analyzed, when the company exchanges conventional devices for high performance inspection instruments. In addition, the sensitivity analysis analyzes the effect of changing the probability of repair, meaning that the company modifies the remedial action codes. Since failure cost can definitely affect the optimization in this type of approach, sensitivity analysis also clarifies the influence on the expected total cost.

Chapter 5 presents the conclusions of the research and proposes further research recommendations.

Chapter 2: Review

● Optimization of inspection/repair for civil structures
● Railroad maintenance

Chapter 3: Methodology

● LEFM analysis to predict crack size
● FORM analysis to evaluate the rail reliability
● ET analysis to perform inspection/remedial actions
● LCC analysis to assess the economical issues

Chapter 4: Application

● Optimization of the number of inspections
● Sensitivity analysis for inspection devices and remedial actions

Chapter 5: Conclusion

● Conclusions
● Recommendations

Fig. 1.6 Organization of Thesis

Chapter 2

Literature Review

2.1 Introduction

This chapter presents a literature review for optimization of inspection/repair intervention in civil structures, such as bridges and offshore structures. The first paper describes the framework of optimization for a reinforced concrete bridge, considering deterioration due to bar corrosion. The second paper refers to offshore structures using another method to decide the timing and areas of inspections appropriate for those structures.

In addition to the literature regarding optimization of inspection/repair in civil structures, two papers on railroad maintenance are discussed. The first of them describes Condition-Based Maintenance (CBM) for rolling stock. CBM is the maintenance strategy

by which maintenance is undertaken only when a component in the system reaches a particular state of deterioration. The final paper refers to rail fatigue analysis and combines laboratory data with field data to improve the conventional Miner's law approach.

2.2 Bridge Structures

The work of Frangopol et al. (1997) provides a conceptual framework for reliability-based LCC design of deteriorating concrete structures. In this approach, reinforced concrete T-girders subject to corrosion are used. The results demonstrate the feasibility of optimizing the inspection/repair strategy for bridges. Some researchers such as Mori and Ellingwood (1984) and Thoft-Christensen and Sorensen (1987) propose the same methodology of evaluating the reliability of structures and optimizing the inspection/repair strategy. However, their works do not cover all, for example, several aspects such as effects of inspection methods, degrading rate over time, and costs of failure. These aspects are important to make the inspection/repair strategy robust and reliable. Frangopol et al. expand the way to optimize the inspection/repair strategy Mori and Ellingwood postulate into the real bridges.

First of all, Frangopol et al. point out that much repair maintenance in highway bridges is based on experience and local practice rather than on sound theoretical investigations, while guidance for routine maintenance exists. A maintenance strategy

supported by only engineering experience is not necessarily better. Therefore, they insist that the reliability should be evaluated by the probabilistic method. They employ a Limit State Equation (LSE) of time-varying bending moment capacity in the second moment analysis to calculate the failure probability using the MCS technique.

Next, as an effect of the inspection method, the capability of inspection is taken into account. In general, the detectability depends on the type of inspection device and the nature of defects in structures. Instinctively, a high cost device should be more accurate and more capable when compared to an inexpensive one. Frangopol et al. define damage intensity, which represents the degree of existing damage due to the corrosion of a bending bar at arbitrary times in order to quantify a damage detectability function. The damage detectability function, which is a function of damage intensity, is assumed normally to be distributed around 50%-50% chance detection.

Third, Frangopol et al. indicate that a systematic means of structuring and evaluating the repair possibility related to an uncertain inspection/repair environment provided by an Event Tree (ET) analysis. In the study, the ET is used to represent all possible events associated with only repair and no-repair. It is assumed that bridge agents always repair or rehabilitate bridges if defects are detected.

Fourth, a total expected cost including inspection cost, repair cost, and failure cost is evaluated as LCC based on the results of the ET analysis. The LCC is mathematically combined by the probabilistic expected value of each cost. A trade-off appears between a higher reliability and the minimum expected total cost. The goal of an optimal inspection/repair strategy is to minimize the LCC of a given structure while satisfying

33

acceptable reliability level throughout the service life.

Finally, numerical results indicate that the optimal number of inspections is six in a particular reinforced concrete bridge; When the service life is 75 years, failure probability 0.02275 is an acceptable reliability level, inspection cost is 5.4units, repair cost is 115.4units, and failure cost is 50000units. In addition, the influence of changing failure cost and inspection quality is analyzed through the sensitivity analysis.

2.3 Offshore Structures

Onoufriou (1999) presents a study on the development and an application of reliability-based inspection planning technique for offshore structures, such as fixed platforms and jack-up drilling rigs. The general methodology on the structural reliability theory is used to optimize inspection schedule, while reflecting the characteristics of offshore structures. Offshore structures have a lot of welded joints and some joints are underwater where critical live loads are waves and wind. Underwater inspections are used as a means of monitoring the integrity and performance of these offshore structures to ensure their safety and operability. However, these adverse circumstances represent a significant cost to the operators. In a more conventional approach to inspection planning in offshore structures, the various inspection criteria are combined in a qualitative manner to make an inspection plan. Therefore, the industry needs a tool for rationalizing quantitatively the selection of joints for inspections in order to maximize the efficiency of

inspections. Onoufriou set out the following methodology.

The first step is to identify the significant joints to reduce the area of inspections in the way the criterion has fatigue life of less than ten times the service life of the structure. The next step is to perform a probabilistic fatigue analysis to calculate the failure probability of the joints during the service life, using both the linear cumulative damage law and fracture mechanics regarding LSE. The reason two ways is used is that the former is for fatigue life prediction and the latter method is for updating the crack information.

Furthermore, when these reliability levels reach particular values over time, called target level, it is assumed that inspection has to be done. In the case of "no detection," where no crack is detected at that time, it is possible to update the reliability curve to reflect the increased estimation confidence in the performance of the joints by the Bayesian approach. The likelihood function in Bayes' theorem behaves as a kind of filter representing the quality of inspection technique. When performing inspection updating for "crack detected," where a defect is found, the subsequent inspection interval reduces as detected cracking size increases. It is to be expected that the information obtained from the inspection shows that cracks have propagated faster than originally anticipated and the information is reflected in crack growth prediction in the future.

The procedure is repeated until optimizing the number of inspections. Target reliability level, where an inspection is supposed to be done, can typically be determined by taking into account the magnitude of failure consequence. If the consequence is very serious for the intact structure, the high target reliability level is adopted; otherwise, the

lower level is employed. Offshore structures have many welded joints, alluded to before, making their redundant against failure. Onoufriou also determines the target reliability level derived from the redundancy analysis. The target values are important parameters in this type of analysis, so that the determination of the value deserves careful consideration.

Onoufriou finally mentions that these methods are not intended to replace the more traditional approach and engineering judgement as the conclusion. The methods are regarded as an additional tool to make more rational decision to be made on inspection planning with significant safety and cost benefit.

2.4 CBM Applied to Rolling Stock

Ma (1997) proposes a maintenance strategy based on the CBM technique to decide the optimal replacement condition by minimizing the LCC and applies the method to rolling stock maintenance. CBM is the maintenance strategy by which the maintenance is undertaken only when a component in the systems reaches a particular state or condition of deterioration. The key issue when implementing CBM is the accuracy of the inspection, because CBM allows car shop engineers to decide the timing of replacement of the components based on the condition that the inspection indicates.

Since, for many practical reasons, the car shop engineers usually perform only external inspection for rolling stock, it is essential to estimate the internal condition from the results of that external inspection. Ma follows the performance threshold method,

which consist of an evaluation of system and random parts, to predict the internal condition from the external condition. Even though the statistical forecast technique is applied, the results inevitably have errors. Ma compensates the errors with sensitivity and specificity method, usually used in epidemiological study. Finally the research addresses a LCC model, which evaluates all economic issues including initial cost, installation cost, salvage cost, and failure cost. As a result, Ma proposes rolling stock should be inspected at 0.4-condition limit state, which is the nominal value, under both perfect and imperfect inspection techniques.

2.5 Rail Fatigue Analysis

The research of Shyr (1993) enhances the Phoenix model developed by the Association of American Railroads (AAR), a conventional rail fatigue analysis model based on Miner's damage accumulation law, by combining field data with laboratory data. Since the Phoenix model had been developed on the basis of theories of material behavior and laboratory results only, it has been used primarily as a supplemental tool to analyze rail fatigue. Shyr develops his improved model using the Bayesian updating method to combine both data sources, considering all types of rail defects in the railhead including transverse defects and split head defects.

Shyr formulates a hazard rate function to predict rail fatigue life, using previous results and assuming that rail fatigue follows the Weibull distribution. Current railroads

are sometimes welded, so that rail fatigue needs to be set up for welded rail in addition to traditional joint rails. The formulation uses the Poisson approach for spatial aggregation of rail units in the welded track.

Finally, Shyr draws comparison parameters between the Phoenix model and his model by using the t-statistics method. It turns out that the Phoenix model underestimates the scale of transverse defects and overestimates the scale of split head defects to predict fatigue defects. Hence, the Phoenix model does not always accurately represent actual situations.

2.6 Summary

Based on the literature review, it is found that the structural reliability theory can predict the reliability level when considering the uncertainty of inspection devices and remedial actions. In addition, the ET and LCC analysis can optimize the number of inspections during the service life. When applying the structural reliability theory to other structures, it is important to tale into account the unique characteristics of those structures, such as load condition, inspection devices, and decision-making process. Furthermore, through the literature review of railroad maintenance, it turns out that CBM can not take into account the uncertainty of deterioration models, and the conventional method for rail fatigue analysis can not reflect the results of in-service inspections, even if enhanced by using several statistics approaches.

Chapter 3

Reliability-Based Optimization of Rail Inspection

3.1 Introduction

This chapter presents a methodology developed for the application of LEFM analysis, FORM analysis, ET analysis, and LCC analysis in order to investigate optimization of rail inspection/repair intervention. The outputs from the LEFM analysis are used for the FORM analysis to evaluate the reliability profile of a rail at arbitrary times, taking into account deterioration due to the rail base crack. The ET analysis presents systematically all possible events and actions which track engineers can take. The LCC analysis shows the total expected cost regarding rail defect management based on the ET analysis.

39

3.2 LEFM Analysis

3.2.1 Crack Growth Model

In general, many fatigue life analyses have applied the Miner's damage accumulation law or some specific PDFs such as the Weibull and Exponential distributions, to predict the probabilistic life of a metallic material, since the models accordingly represent the characteristics of the material. However, railroad companies usually use a crack size as the inspection results. Therefore, it is hard to deal with reflecting the results of the inspections and repair strategy in their approaches because they do not provide information about crack size. A quantitative analysis for the rail reliability needs the knowledge of the crack size at arbitrary times, so a crack growth model based on LEFM is employed instead of the Miner's damage accumulation and a specific PDF model in this thesis.

The crack growth model used in this study is based on the Paris and Erdogan's law, where the rate of crack growth is defined as

$$\frac{da}{dN} = C(\Delta K)^m \qquad (3.1)$$

where, a is the crack size, N is the number of the stress cycles, C and m are material parameters, and ΔK is the stress intensity factor range. According to LEFM under a constant amplitude loading, ΔK can be estimated as

$$\Delta K = K_{max} - K_{min} = YS\sqrt{\pi a} \qquad (3.2)$$

where, Y is the geometric correction factor and S is the tensile stress range, also called the far-field stress range.

It is noted that the use of the stress intensity factors implies that equation (3.1) only applies to essentially elastic situation, so that the factor provides a reasonable description of the crack tip stress field for a distance up to $0.1a$ from the crack tip.

3.2.2 Bending Moment and Stress at Rail Base

The application of LEFM to surface defects requires knowledge of the stress intensity factor. The stress intensity factor is generally a function of stress amplitude as described in the previous section. Hence, it is essential to evaluate the stress amplitude in the LEFM analysis.

The track consisting of rails, ties, ballasts, and a roadbed can be designed as the continuously supported elastic model as depicted in Fig. 3.1. The equation to express rail displacement applied by trainloads can be set up by a forth-order differential equation described as

$$EI\frac{d^4y}{dx^4} + ky = 0 \tag{3.3}$$

where, E is the Young's modulus of the rail, I is the second moment of area of the rail, x and y are the axes in the two dimensional coordinates, and k is the spring coefficient at the rail support, which indicates elasticity of both ties and ballasts (Sato 1997). The second-order integral of the equation (3.3) indicates the bending moment of a rail base under the following boundary condition:

41

$$x = 0 \Rightarrow \frac{dy}{dx} = 0 \tag{3.4}$$

$$x = 0 \Rightarrow 2EI \frac{d^3 y}{dx^3} = W \tag{3.5}$$

$$x \to \infty \Rightarrow y \to 0 \tag{3.6}$$

hence, the bending moment can be expressed as

$$M_i = -EI \frac{d^2 y}{dx^2} = \frac{W}{4\left(\dfrac{k}{4EI}\right)^{0.25}} \cdot \exp\left[\left(\frac{k}{4EI}\right)^{0.25}\right] \cdot \left(\cos\left(\frac{k}{4EI}\right)^{0.25} x - \sin\left(\frac{k}{4EI}\right)^{0.25} x \right)$$

$$\tag{3.7}$$

here, W is the trainload. k, the spring coefficient at the rail support, can be defined as

$$k = \frac{1}{\dfrac{1}{K_1} + \dfrac{1}{K_2}} \cdot \frac{1}{d} \tag{3.8}$$

where, K_1 is the comprehensive spring coefficient of a tie both considering the tie bending and compression, K_2 is the spring coefficient of ballasts, and d is the tie interval. K_1 can be expressed as

$$K_1 = \frac{1}{\dfrac{1}{K_a} + \dfrac{1}{K_b}} \tag{3.9}$$

here, K_a is the spring coefficient of the rail pad and K_b is the spring coefficient of the tie bending obtained by solving another differential equation. K_a is equal to 49 [kN/m], K_b is equal to 202.6 [kN/m] and K_2 is equal to 22.2 [kN/m] based on the rail track engineering. Consequently, k is 22.15 [MPa].
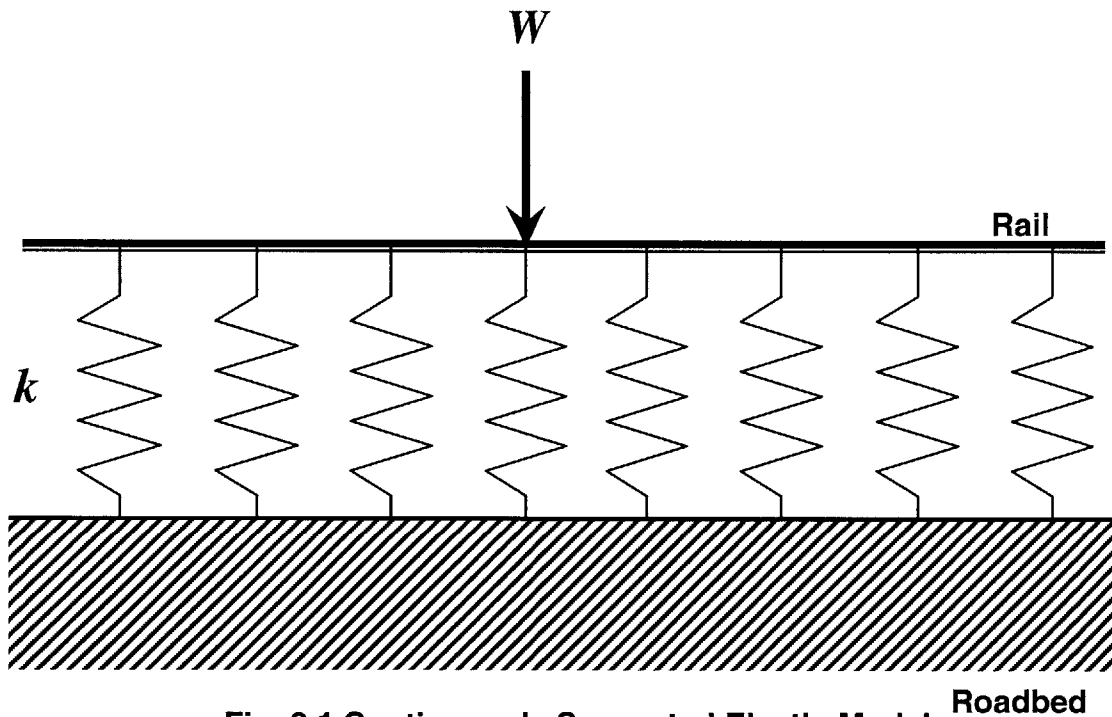
Fig. 3.1 Continuously Supported Elastic Model

The bending moment at a particular point in a rail base caused by trains is calculated based on the superposition method because of the linearity. Therefore, the total bending moment can be expressed as

$$M = \sum_{i=1}^{l} M_i \qquad (3.10)$$

where, M is the total bending moment, M_i is the moment caused by each wheel load, and l is the number of wheel. Since recent rolling stock has bogie trucks, Fig. 3.2 can model trainloads, where each wheel load is 10 [t]. The fixed distance between axes is around from 1.9 [m] ~2.3 [m] (Yazawa 2000); here 2.0 [m] are employed. Next bogie truck is more than 10 [m] apart, so that the influence of the trainload for the area of

43

interest can be neglected. The total bending moment is divided by the modulus of section to evaluate the stress. Fig. 3.3 shows the result when train speed is 100 [km/h]. As shown in the graph, in addition to the expected tensile stress that occurs when the trainload passes directly over the simulated point of measurement, there is also compression stress. The compression stress occurs just before and just after the trainload passes. The compression stress is one third of the tensile stress. Consequently, the stress amplitude is 50 [MPa] at the maximum. The modulus of section of general rail, 50N used in JR East is 2.739E-4 [m^3], and the rail flexural rigidity is 4.12E-9 [tm^2]

The above result derives from not dynamics but statics. Actual mechanics by the trainload is dynamic and it is known that the dynamic stress is greater than the static one due to the concavity and convexity of rail/wheel as well as rail irregularities. Therefore, in order to describe the phenomenon in this thesis, it is assumed that the stress due to the trainload consists of two components, which are the static stress and dynamic stress and the stress can be broken down as

$$\sigma = \sigma_S + \sigma_D \tag{3.11}$$

where, σ is the stress, σ_S is the static stress, and σ_D is the dynamic stress.

This model has advantage of treatability. If both the static and dynamic stress follow the stationary Gaussian random process, the stress amplitude follows Rayleigh distribution. The stress intensity factor range can be the distinction between the maximum and the minimum value of the stress intensity factor under a constant amplitude stress. As a matter of course, the stress intensity factor associated with a variable amplitude stress is different from that calculated under a constant amplitude stress, discussed in detail later.
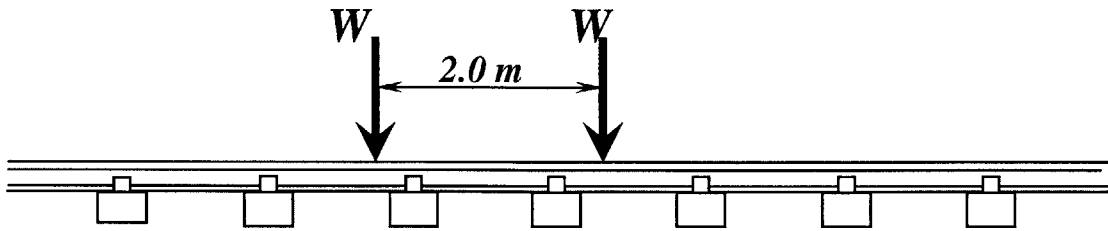
Fig. 3.2 Trainload Model
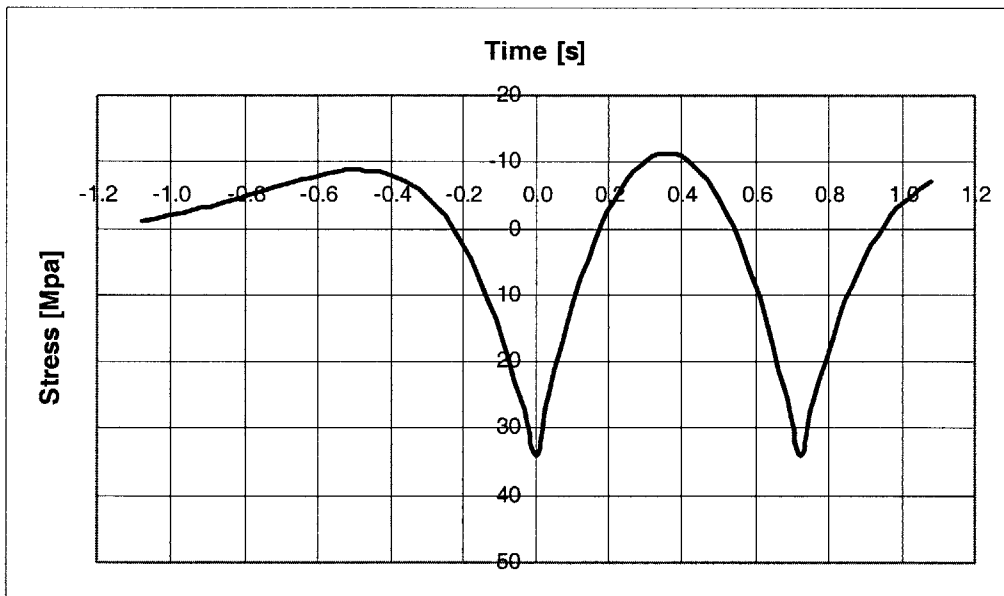
Fig. 3.3 Rail Base Stress Caused by Trainload

3.2.3 Semi-Elliptical Crack Model

Fatigue failure is initiated by an imperfection of materials or from tiny cracks inside the materials. Cracks grow due to cyclic loads applied to the material. As for rail fatigue, rail defects in JR East are generally classified as: 1) traverse defects in the rail head; 2) longitudinal defects in the rail head; 3) surface defects in the rail head; 4) surface defects in the rail head; 5) web defects; 6) base defects; 7) joint-hole defects. This study focuses on the fatigue related to defects in the base area since base defects have been recently responsible for more than 50% of the reasons for the rail broken in JR East as shown in Fig. 1.4 and also for simplifying the analysis.

It is believed that base traverse defects in rails start from a surface imperfection, which is a fabrication crack in the steel. Impacts of wheel and bending stress initiate growth of base separation around the tiny imperfection. Natural crack occurring in practice are often initiated at corners and edges. They tend to grow inwards and assume to be semi-elliptical shape. Therefore, the semi-elliptical crack model is employed to represent base defects of rails with the aspect ratio, $a/c = 1.0$ in this thesis as shown Fig. 3.4. The stress intensity factor in the semi-elliptical crack model can be defined as

$$K = \frac{1.12\sigma(\pi a)^{0.5}}{\xi} \qquad (3.12)$$

here, σ is the far-field stress, a is the crack size, and ξ is an elliptical integral of the second kind, given by

$$\xi = \int_0^{\pi/2} \left(1 - \frac{c^2 - a^2}{c^2}\sin^2\varphi\right)d\varphi \qquad (3.13)$$

where, a and c are defined in Fig. 3.4. If a/c is less than one, the value is approximated by the following equation (Pook 2000).

$$\xi \approx \left(1+1.464\left(\frac{a}{c}\right)^{1.65}\right)^{0.5}$$ (3.14)
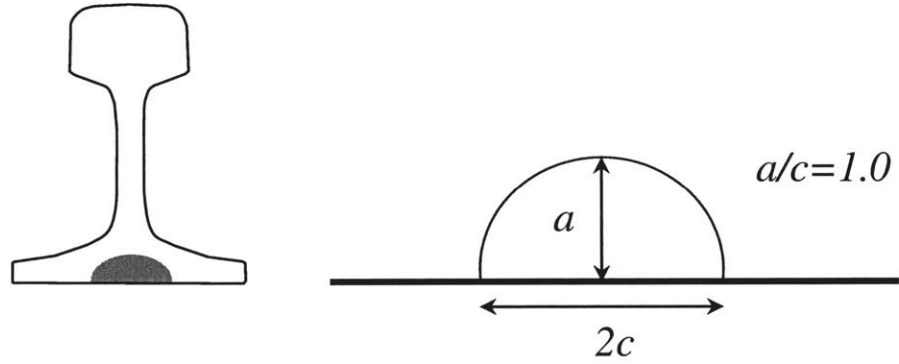
Fig. 3.4 Semi-Elliptical Crack Model

3.2.4 Fatigue Damage Accumulation Function

Integrating equation (3.1) after substituting equation (3.2) for equation (3.1) from a_1 to a_2 corresponding to the number of stress cycle N_1 and N_2, one obtains

$$\int_{a_1}^{a_2}\frac{1}{Y(\pi a)^{0.5}}\,da = \int_{N_1}^{N_2}CS^m\,dN$$ (3.15)

According to Madsen (1985), a function reflecting the damage accumulation from crack size a_1 to a_2 can be defined as

$$\Psi(a_1,a_2)=\int_{a_1}^{a_2}\frac{1}{Y(\pi a)^{0.5}}\,da$$ (3.16)

47

This damage accumulation function is related to the load accumulation by

$$\Psi\left(a_1, a_2\right) = C \overline{S^m} \left(N_2 - N_1\right) \tag{3.17}$$

where, $\overline{S^m}$ is the mean stress-range effect, which is an m-order moment of the PDF of

a stress amplitude parameter (Haldar 1994).

An actual rail is usually subjected to a variable amplitude load process as alluded

to before. Two possibilities are the cycle-cycle counting and the mean stress-range effect

method to consider the fatigue under a variable amplitude stress. The method to count

step-by-step each stress occurred in a rail is not practical. The mean stress-rang effect

method might be appropriate to the study for the fatigue damage accumulation in rails.

The mean stress-range effect can be evaluated as

$$\overline{S^m} = \int_0^\infty s^m f_S(s) \, ds \tag{3.18}$$

where, $f_S(s)$ is the PDF of the stress range parameter, S which is assumed to follow

the stationary Gaussian random process. For rails, the Rayleigh distribution would be the

most appropriate for estimation of S since the trainload stress can comprise of two

components: one is static and the other is dynamic stress as indicated in the section 3.1.2.

If the stress range parameter follows a Rayleigh distribution, the mean stress-range effect

can be shown as follows:

$$\overline{S^m} = \left(S_0 \sqrt{2}\right)^m \Gamma\left(\frac{m}{2} + 1\right) \tag{3.19}$$

where, Γ is a gamma function, and S_0 is a statistical parameter expressed as

48

$$S_0 = \overline{S}\sqrt{\frac{2}{\pi}}$$

(3.20)

where, $\overline{S}$ is the mean value of S, which is 50 [MPa] calculated in the section 3.2.2

3.3 FORM Analysis

3.3.1 Hasofer-Lind Reliability Index

Not only fatigue but also strength of materials is so sensitive that they are statistical by nature. In addition, it is intricate to evaluate the meticulous probability of the failure in materials applied to cyclic loads at arbitrary times. Even if estimated, the results can be much widely varied. Therefore, instead of the rail safety evaluated by rigorous probabilistic prediction of failure, a kind of index that is the Hasofer-Lind reliability index: beta assesses the reliability of rails in this thesis.

This thesis mainly focuses on the issue of reliability using the probability theory. Hence, the probabilistic reliability analysis is discussed in detail in this section. The structural reliability theory is concerned with rational treatment of uncertainties in structures and with the method for assessing the safety and serviceability in structures. The uncertainties are usually described as a random variable vector $\underline{X} = (x_1, x_2, ..., x_n)$.

In the basic concept from the classical structural reliability theory proposed by Cornell (1969), a random variable vector relevant to loads and resistance parameters in structures and functional relationship among them are required. The relationship can be

expressed as

$$Z = g(x_1, x_2, ..., x_n) = g(\underline{X}) \qquad (3.21)$$

This function is called the LSF. The failure surface, which is in a limit state of the structures, is called the Limit State Equation (LSE), and it can be defines as

$$g(\underline{X}) = 0 \qquad (3.22)$$

Geometrically, the LSE is an n-dimensional surface. One side of the failure surface is the safe state, $g(\underline{X}) > 0$ whereas the other side of the failure surface is the failure state, $g(\underline{X}) < 0$. Hence, if the joint PDF of the variables, $x_1, x_2, ..., x_n$ is $f_{X_1, X_2, ..., X_n}(x_1, x_2, ..., x_n)$, the probability of failure: p_f can be defined as

$$p_f = \int \cdots \iint_{X_1, X_2, ..., X_n < 0} f_{X_1, X_2, ..., X_n}(x_1, x_2, ..., x_n) \, dx_1 dx_2 \cdots dx_n \qquad (3.23)$$

this is rewritten for brevity by the volume integral of $f_{\underline{X}}(\underline{x})$ over the failure region as

$$p_f = \int_{g(\underline{X}) < 0} f(\underline{x}) \, d\underline{x} \qquad (3.24)$$

In general, solving the integrals from the above equation is a complicated process and can be done in a closed form only for a simple case. Moreover, the calculation of multi-dimensional integral requires the information of the joint PDF or each PDF of the variables. For practical reasons, the information is often unavailable or too difficult to obtain on sufficient data. Therefore, some alternative methods are needed in order to evaluate the probability of failure. These methods can be either analytical or numerical. Analytical methods to represent the reliability as a reliability index: beta. One of them is the First-Order Second Moment (FOSM) method based on determining mean

and variance of the variables. Numerical methods evaluate directly the reliability through simulations, such as the Monte Carlo Simulation and the Latin Hyper Sampling.

The concept by Cornell has an invariance problem that the results change by the way to define a LSF. Hence, Hasofer-Lind (1974) improves the concept to the FORM. The reliability index: beta is defined as the minimum distance from the origin to a failure surface of a space defined with the random vectors in this approach. The most probable point (MPP) of failure, the design point, is found in a standard normal space $\underline{U}$ for a single failure driven LSE. The components of $\underline{U}$ are normally distributed with zero means and unit variance and are statistically independent. Any set of continuous random vectors can be transformed into $\underline{U}$ using the equivalent normal variables (see Appendix A). The MPP u^* also lives on the hyper surface and the location is the closest point on the LSE to the origin in $\underline{U}$-space. The MPP can be found by figuring out the following constrained optimization problem .

$$
\begin{aligned}
Minimize \quad & D = \sqrt{\underline{U}^T \underline{U}} \\
s.t. \quad & g(\underline{u}) = 0
\end{aligned}
\tag{3.25}
$$

where, D is the distance from the origin to the MPP, and T is transpose notation. Although various algorithms exist to perform the MPP search, one of them is the Rackwitz-Fieesler (1978) algorithm, which is based on Newton-Raphson root solving recursive approach. The formula is defined as

$$
\underline{u}_{k+1} = \frac{1}{\left| \nabla g(\underline{u}_k) \right|^2} \left[\nabla g(\underline{u}_k)^T \cdot g(\underline{u}_k) - g(\underline{u}_k) \right] \nabla g(\underline{u}_k)
\tag{3.26}
$$

here, $\underline{u}_{k+1}$ is the MPP at the (k+1)th iteration, $\nabla g(\underline{u}_k)$ is the gradient vector of LSE at

$\underline{u}_k$, kth iteration point (see Appendix B). When the LSE is nonlinear, the gradient is not constant and varies from one point to another point. Hence, the MPP has to be searched through the recursive formula given by equation (3.26). If the LSE is linear, FORM can give a correct value regarding probability of failure.

The algorithm is repeated until convergence satisfying the following criteria

$$If \quad |g(\underline{u}_k)| \leq \varepsilon, \ stop \qquad (3.27)$$

where, ε is a small quantity as 0.001, which is employed in this thesis. After transformation by two-parameter equivalent transformation, the reliability index is directly related to the probability of failure: p_f described as

$$p_f = \Phi(-\beta) \qquad (3.28)$$

where, $\Phi(\bullet)$ is the cumulative function of the standard normal variate.

3.3.2 Rail Reliability Analysis of the LEFM Approach

Rail defects directly relate to the serviceability of tracks so that the limit state of serviceability exists on a state of crack growth. When the critical crack size, a_C is specified, a LSF for rails subjected to N stress cycle can be defined as

$$Z = g(\underline{X}) = a_c - a(N) \qquad (3.29)$$

where, $a(N)$ is a crack size after a rail is subjected to N stress cycle. A crack size corresponding to the number of stress cycles can be obtained by the Paris and Erdogan's kinetic crack growth law as discussed earlier. Once $a(N)$ exceeds the critical crack size,

rail can be considered as failure.

Since the function $\Psi(\bullet)$ defined by equation (3.16) is monotonically increasing with the crack size a, the LSE represented in equation (3.29) can be expressed as

$$\Psi(a_c, a_0) - \Psi(a_N, a_0) = 0 \qquad (3.30)$$

using equation (3.17), the above LSF can be rewritten as

$$\Psi(a_c, a_0) - C\overline{S}^m(N - N_0) = 0 \qquad (3.31)$$

where, a_0 is the initial crack size, and N_0 is the crack initiation period.

The initial crack size is the crack size from which the fatigue crack will propagate. It is a lower limit for the crack size which can be a fabrication crack. The large variability in a fatigue analysis can be attributed to the uncertainty in the initial crack size, which is usually random variable.

Although many types of the PDF of initial crack size in modeling the uncertainty are suggested, in this study, it is modeled to a lognormal distribution with the mean of 0.2 [mm] and the correlation of variance (COV) of 0.3. The crack initiation period, N_0 is another aspect of crack initiation. It seems that no reasonable theory exists for the period, some models are proposed. For simplicity, however, it is assumed that N_0 is equal to zero in this thesis. Through the methods mentioned in the section 3.2 and 3.3.1, the reliability index of rail is evaluated.

The critical crack size a_c is a significant parameter in the LEFM formulation. It can be defined as the crack size causing failure of rail or the design crack size beyond which the serviceability requirements cannot be satisfied. Since the fracture toughness is

53

38 [MPa m$^{0.5}$] in general rail materials in JR East, the kinetic crack growth law shown in equation (3.12) describes the critical crack size as

$$a_c = \frac{1}{\pi}\left(\frac{K\xi}{1.12\sigma_c}\right)^2 \tag{3.32}$$

where, σ_c is the critical far-field stress.

Rails generally have residual stress due to the manufacturing process. Kashiwaya (2000) performs laboratory experiments to evaluate the internal residual stress in detail by stress relaxing method with bar strain gage. As a result of the examination, it turns out that large tensile residual stress exists at a rail base, which is around 100 [Mpa]. Because rails extend in summer and shrink in winter due to the effect of the temperature variation, thermal stress should be also taken into account to evaluate the total stress. The tensile stress of rails accompanied with decreasing temperature is at most 30 [Mpa] from the theoretical solution (Sato 1997). Since the compression stress applied by trainloads is no more than 10 [Mpa] as shown in Fig. 3.3, crack closing process by the compression stress can be ignored. In consequence, the tensile stress is always applied to the rail base. The critical crack size is 25 [mm] corresponding to the maximum stress, which can be 180 [MPa]. Fig. 3.5 shows the relationship between the far-field stress and the critical crack size. The critical crack size has uncertainties due to the model, materials, and environment so that the critical crack size is also random variables. It is assumed that the critical crack size follows a lognormal distribution.

Based on the literature (Kashiwaya 2000), the means of C is 1.0E-11 and of m is three in general rail materials in JR East. Table3.1 summarizes the parameters in

this FORM analysis. Fig. 3.6 shows the relationship between the stress cycle and the

simulated reliability index.
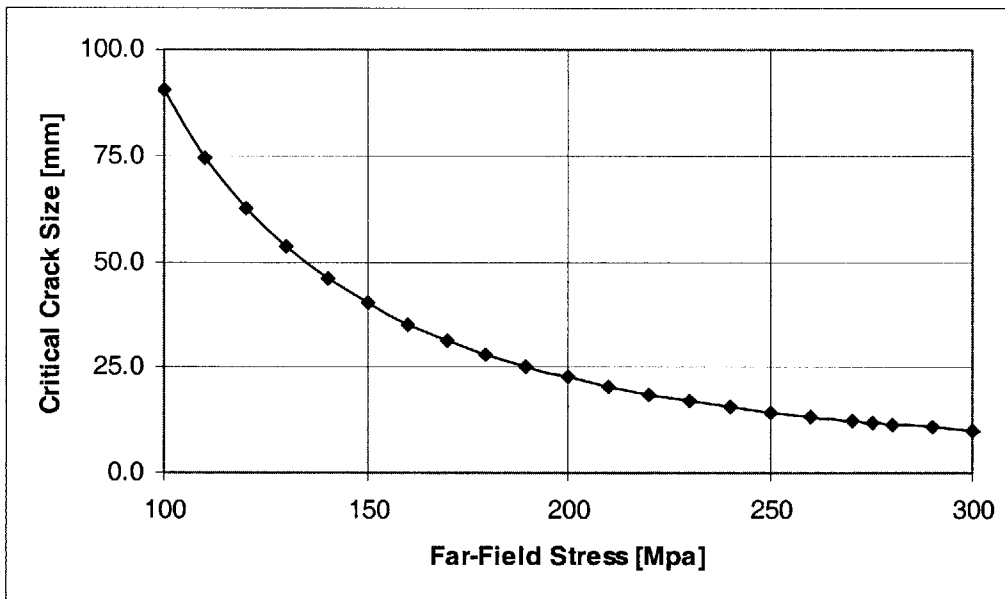
Fig. 3.5 Relationship between Critical Crack Size and Far-Field Stress
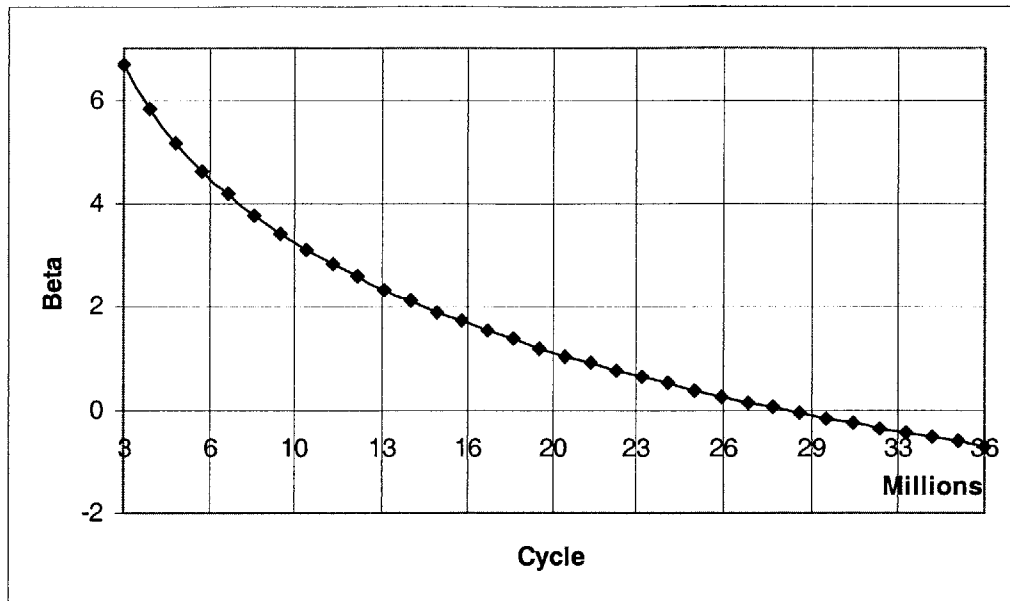
Fig. 3.6 Relationship between Stress Cycle and Beta

Tabale3.1 Statistical Characteristics of Variables for FORM Analysis

Variables	Notation	Type	Mean Value	COV
Critical Crack Size	a_c	Lognormal	25 [mm]	0.1
Initial Crack Size	a_0	Lognormal	0.2 [mm]	0.3
Material Parameter	m	Constant	3.0	-
Material Parameter	C	Lognormal	1.0E-11	0.3

3.3.3 Verification of Reliability Index

As alluded to the section 3.3.1, FORM performs the correct probability of failure, when the LSE is linear. However, LSEs can be nonlinear in many cases due to the nonlinear relationship among the random variables in the LSE, or due to some non-Gaussian variables. The linear approximation of a nonlinear LSE is equivalent to replacement of an n-dimensional failure surface with a hyper-plane tangent at the MPP as shown in Fig. 3.7.

In other words, the curvature of the nonlinear LSE is ignored in the FORM approach, which uses only a first-order approximation at the minimum distance point. The FORM has errors when calculating the reliability index as long as the LSE does not have linearity. However, the accuracy of the second-moment linear approximation is generally difficult to assess, because this will depend on the degree of non-linearity of the LSE. Therefore, a large sample MCS verifies the reliability index calculated in the FORM analysis.

MCS approach consists of drawing samples of the variables according to their PDF and then feeding them into a mathematical model of the LSF. The samples obtained would give the probabilistic characteristics of the response of the random variable of the LSF. It is known that if the value of the LSF is less than zero, it indicates failure. Let M_f be the number of simulation cycles, when the LSE is less than zero. Let M be the total number of simulation cycles. Therefore, an estimation of the probability of failure: p_f can be expressed as

57

$$p_f = \frac{M_f}{M}$$

(3.33)

It is obvious that the estimation would converge to the true value as M approaches infinity. Therefore, MCS includes errors as long as M is a limited number. The way to evaluate the error associated with the number of simulation cycles is by approximating the binomial distribution with a normal distribution and estimating a 95% confidence interval of simulated probability of failure (Shooman 1968). It can be shown that

$$P_r\left[-2\sqrt{\frac{(1-p_f)p_f}{M}} < \frac{M_f}{M} - p_f < 2\sqrt{\frac{(1-p_f)p_f}{M}}\right] = 0.95$$

(3.34)

where, p_f is the true probability of failure. The percentage error can be defined as

$$\varepsilon \ [\%] = \sqrt{\frac{1-p_f}{M \cdot p_f}} \times 200 \ [\%]$$

(3.35)

Table3.2 shows the results where sample size is equal to two millions, when load cycle N is 10, 20, and 30million. They are 95% likely that the actual probability will be within

$$N = 10 \, Million; \ 3.095 < \beta < 3.122$$
$$N = 20 \, Million; 1.052 < \beta < 1.057$$
$$N = 30 \, Million; -0.153 < \beta < -0.157$$

(3.36)

Fig. 3.8 shows the distinction the results between FORM and the MCS. As a matter of the results, FORM is appropriate to evaluate the reliability index in this research.
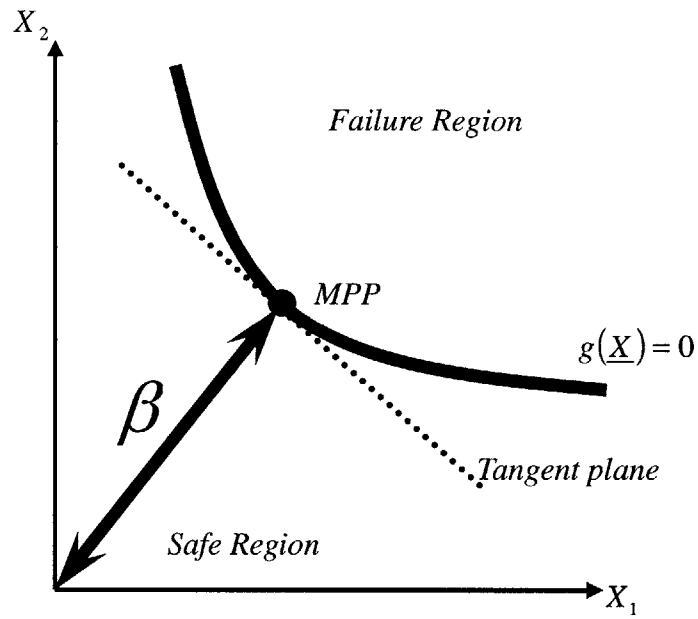
Fig. 3.7 Tangent Plane to $g(\underline{X})=0$ **at MPP**

Table3.2 Results of Monte Carlo Simulation

Stress Cycle	M_f	p_f	ε
10000000	1882	9.41E-4	4.608 %
20000000	291651	1.458E-1	0.342 %
30000000	1123345	5.617E-1	0.125 %
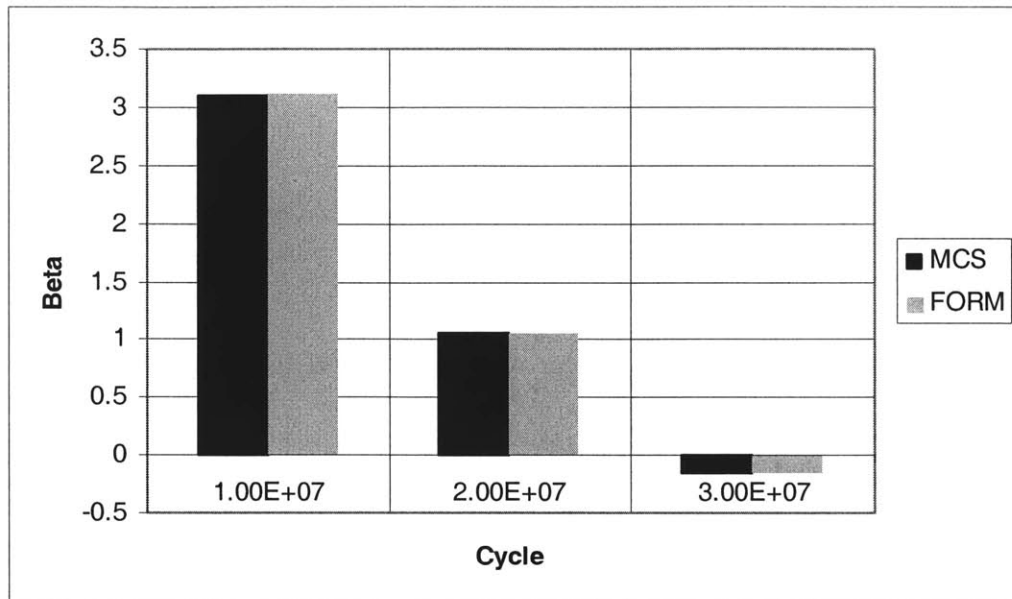
Fig. 3.8 Distinction of Results between FORM and the MCS

3.4 ET Analysis

3.4.1 Event Tree Model

An ET provides a systematic means of structuring relevant events related to an uncertain environment. It represents the direct relationship and provides a clear and precise definition among all possible events.

The ET is used as a model to represent all possible events associated with inspection/repair actions, which are detection/repair, detection/no-repair, and no-detection in this thesis. In order to make up an ET, a decision of above three options needs to be made after every inspection. After every new inspection, past remedial actions affect new

remedial actions. Hence, if no crack is detected or the crack size can be tolerated, no-repair action would be taken. If repair work is assumed to be performed only when a crack is detected and the crack size exceeds a critical repair level, a_r, the total number of braches in an ET is 3^N, where N is the number of inspections during the service life.

Fig. 3.9 shows the basic component, which consists of chance nodes and folks, of the ET. It represents the first mutually exclusive set of chance events. At the terminus of each branch, track engineers form a new chance nodes and folks. Each probability in these chance nodes is derived from the Probability of Detection (POD) and the Probability of Repair (POR) discussed later.
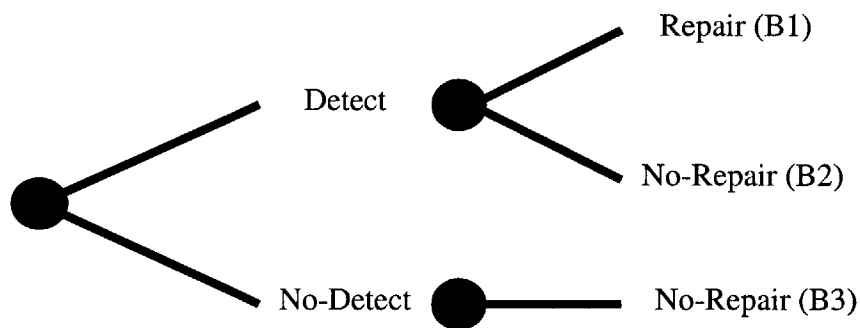
Fig. 3.9 Basic Component for ET

The probability of the consequences, such as B1, B2, and B3 shown in Fig. 3.8, can be calculated as follows:

$$P_r(B1) = P_{b_1} = p_{\text{det}} \cdot p_{rep|\text{det}}$$
$$P_r(B2) = P_{b_2} = p_{\text{det}} \cdot \left(1 - p_{rep|\text{det}}\right) \qquad (3.37)$$
$$P_r(B3) = P_{b_3} = \left(1 - p_{\text{det}}\right) \cdot 1.0$$

where, p_{det} is the probability of detecting defects, $p_{rep|\text{det}}$ is the probability of repairing defects given a detection of defects. Since the consequences of both B2 and B3 are the same actions, which is no-repair, Fig. 3.9 can be simplified as shown in Fig. 3.10. The probabilities of repair and no-repair shown in Fig.3.10 are defined as

$$P_r(repair) = p_{\text{det}} \cdot p_{rep|\text{det}}$$
$$P_r(no - repair) = p_{\text{det}} \cdot \left(1 - p_{rep|\text{det}}\right) + \left(1 - p_{\text{det}}\right) \qquad (3.38)$$

For instance, assume that two inspections will be done during the service life. Fig. 3.11 shows its ET. Let R_1^+ indicate that a repair is done at time t_1, and let R_1^- exhibits that a repair is not done at time t_1. Similarly, an action must be taken again whether or not to repair the structure. R_2^+ displays repair and R_2^- indicates no-repair in the second action. Let P_{bi} be the probability of taking b_i branch. Hence,

$$P_{b1} = P_r\left(R_1^+\right)$$
$$P_{b2} = P_r\left(R_1^-\right)$$
$$P_{b3} = P_r\left(R_1^+ \cap R_2^+\right)$$
$$P_{b4} = P_r\left(R_1^+ \cap R_2^-\right) \qquad (3.39)$$
$$P_{b5} = P_r\left(R_1^- \cap R_2^+\right)$$
$$P_{b6} = P_r\left(R_1^- \cap R_2^-\right)$$

The reliability of the structure must be evaluated at time t_1, t_2 and calculate the reliability index of the structure after corresponding to the inspections.

In addition, the weighted effect of each repair of branch must be considered. Above procedures can be generalized into n times inspections. For each branch, b_i the reliability index of a rail at a time point given where b_i is taken, is multiplied by the probability of the branch, p_{b_i}. The expected reliability index is equal to the sum of overall branches and defined as

$$E[\beta(N)] = -\Phi^{-1}\left(\sum_{i=1}^{2^n} \Phi\left(-\beta_i(N)\right) \cdot P_{bi}\right) \qquad (3.40)$$

here, $\Phi^{-1}(\bullet)$ is the inverse function of a cumulative standard normal variate, n is the number of lifetime inspections.
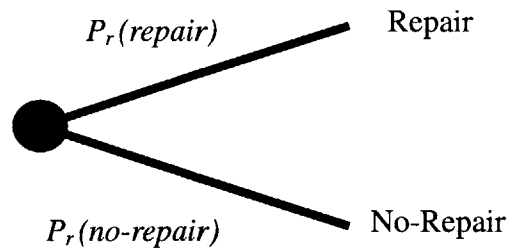
Fig. 3.10 Simplified Basic Component for ET
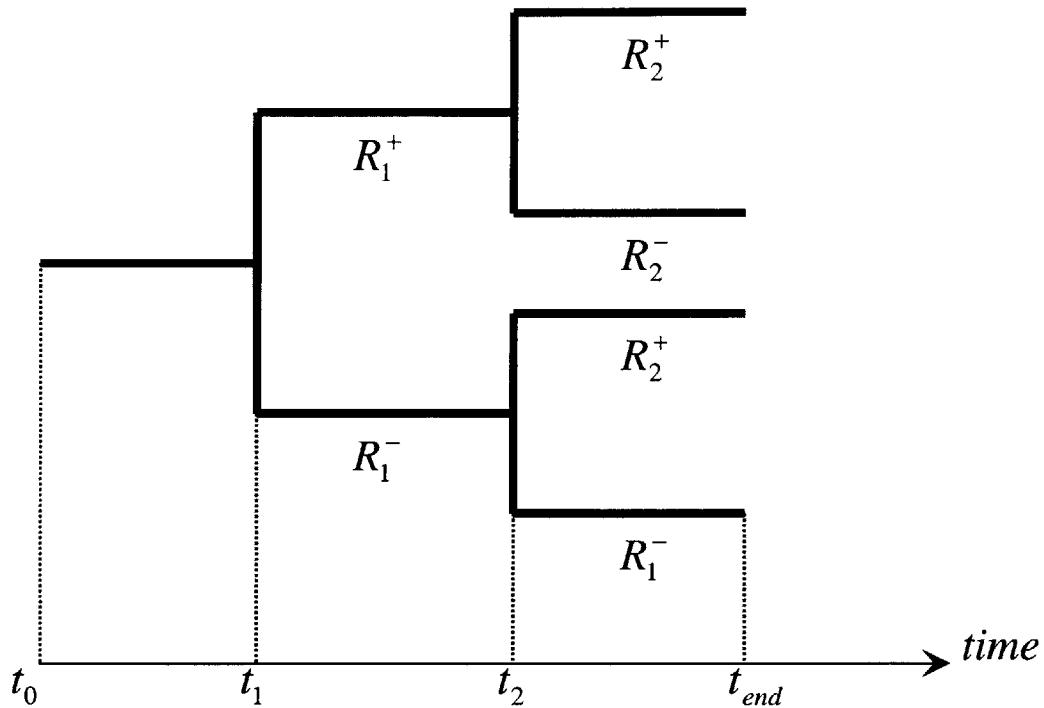
Fig. 3.11 ET for Two Inspections during the Service Life

3.4.2 Uncertainty of Detection

NDT plays an essential role in a condition assessment in-service and repair decision-making process. However, no inspection is perfect. NDT outputs depend on many uncertain factors, such as conditions of structures, environmental conditions during inspection, and operator skills.

Neglecting these uncertainties not only results in misinformed decision-making but also leads to unnecessary remedial actions. A rational approach to evaluate the role of these sources of uncertainties is a probabilistic method. Hence, evaluation of capability of NDT expressed in terms of probability is essential to the ET analysis.

The capability of an inspection technique can be defined in terms of two criteria, detectability and accuracy. The ability of detecting cracks, termed detectability, depends on sizes of cracks and the resolution to the capability of a particular NDT technique adopted. It is known that there is always a critical crack size for a given NDT technique below which a crack cannot be detected. As for accuracy, errors in defects refer to measurement noises with respect to true sizes when defects are detected. The relationship between the actual and measured crack size also depends on types of cracks and attributes of a given NDT technique. The capability of NDT is termed POD in this thesis.

A POD is generally expressed in terms of Cumulative Density Function (CDF). It is expected that as a crack size increases, its detectability also increases. It is assumed that detectability can be described as the mean of CDF and accuracy can be expressed as the COV of CDF in the model.

Zheng and Ellingwood (1998) propose the POD can be modeled to an exponential distribution. Zhao and Haldar (1994) presume that the POD of a crack in metal materials follows a lognormal distribution. In this thesis, the ET analysis is performed on the assumption that POD is lognormally distributed with the mean of 0.5 [mm] and the COV of 0.05 shown in Fig. 3.12.

For any inspection, if the actual crack size at the time of inspection is smaller than a detectable crack size when given NDT technique, the defect is not expected to be detected. The event which no crack is detected during the inspection, when the rail has been subjected to N stress cycle, can be expressed as

$$a_d \geq a(N) \qquad (3.41)$$

65

where, a_d is the capability at the time of inspection, $a(N)$ is the estimated crack size

at N stress cycle. The LSF of the event as no-detection during inspection can be

defined as

$$h(\underline{X}) = \Psi(a_d - a_0) - \Psi(a_N - a_0)$$
$$= \Psi(a_d - a_0) - C\overline{S}^m N$$

(3.42)

where, $\Psi(\bullet)$ is a fatigue-damage function, $\overline{S}^m$ is the mean-stress range effect defined

in the section 3.1.4, N is a number of stress cycle to the corresponding to the time of

inspection. p_{det} can be obtained from solving this LSF based on the FORM,.
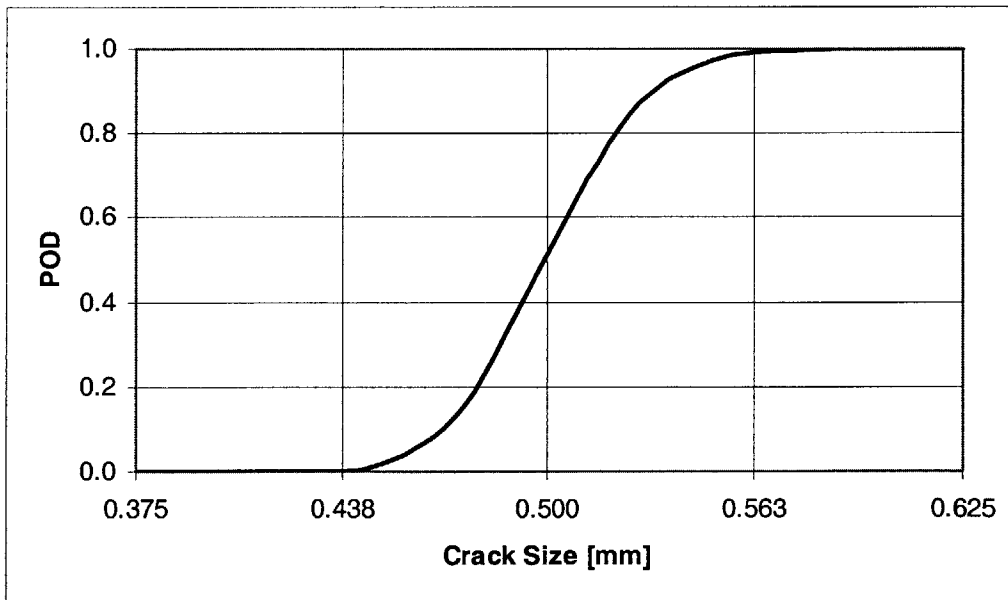
Fig. 3.12 Capability of Inspection

3.4.3 Uncertainty of Repair

Generally speaking, railroad companies have two options to repair damaged rails, when they detect rail defects in a conventional joint rail track. One is to replace the damaged rail; the other is to apply a joint bar. In this thesis, it is assumed that railroad companies have an only option of replacement for simplicity of the analysis. In other words, either decision of replacement or non-replacement will be made after every inspection as long as defects are detected.

JR East defines the codes for rail remedial action shown in Table1.1. This management policy gives two opportunities regarding replacement for the track engineers. One is planning replacement policy and the other is immediate replacement policy corresponding to the critical repair level. The decision about these options can be interpreted in a probabilistic form, Probability of Repair (POR) that implies track engineers' actual response after inspections. It is assumed that the critical repair level, a_r follows a uniform distribution, where the maximum value of the PDF is the code size on which track engineers must replace the damaged rail and the minimum value of the PDF is the size on which the engineers will take some management actions. Fig. 3.13 shows the CDF of a_r. An associated LSF, $i(\underline{X})$ similar to the one employed for reliability analysis described earlier, can be defined as

$$i(\underline{X}) = a_r - a(N)$$
(3.43)

where, a_r is the critical repair level, $a(N)$ is the estimated crack size at N stress cycle. The $p_{rep|det}$ can be obtained by using FORM with respect to the above LSF.

67
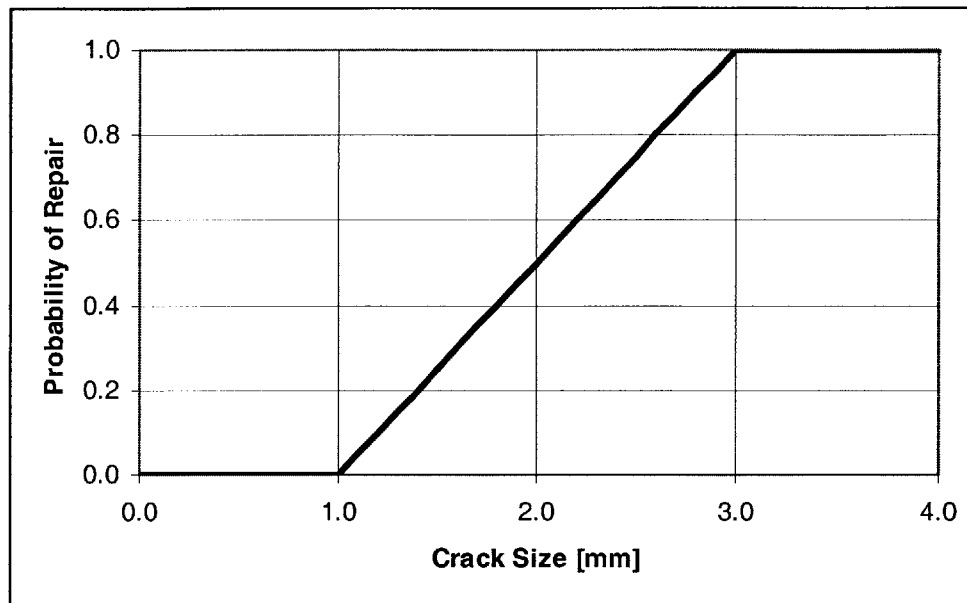
Fig. 3.13 Probability of Repair

3.4.4 Numerical Results

Fig. 3.14 shows the relationship between stress cycles and the expected reliability index based on uniform interval inspection strategy during the service life, 360 Million Gross Ton (MGT) when one inspection case. It is certain that the one inspection/repair intervention improves the reliability. Fig. 3.15, Fig. 3.16, Fig. 3.17, Fig. 3.18, and Fig. 3.19 show the relationship between stress cycles and the expected reliability index, when two, three, four, and five uniformly interval inspections during the service life, respectively.
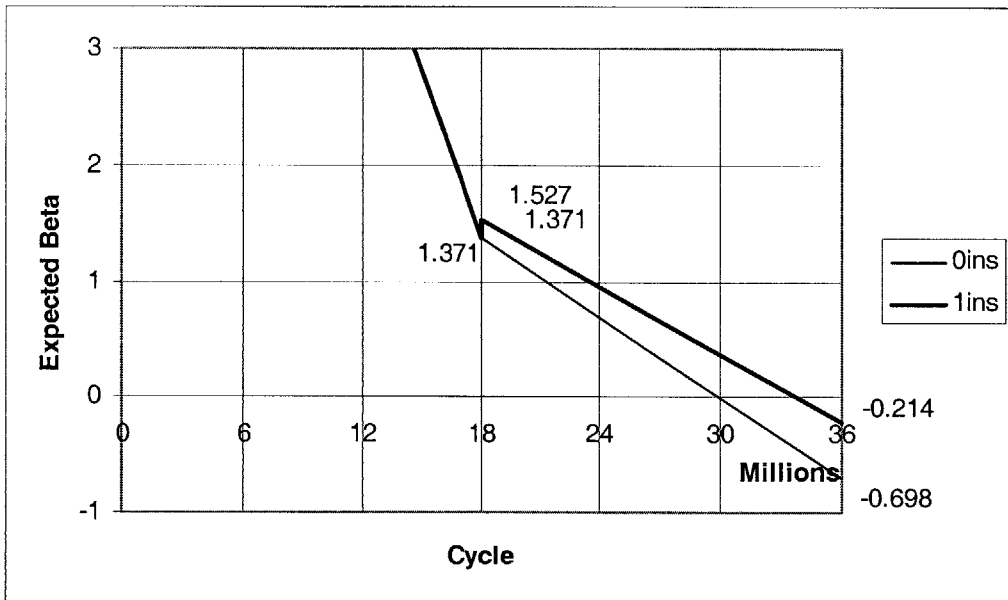
Fig. 3.14 Case of One Inspection
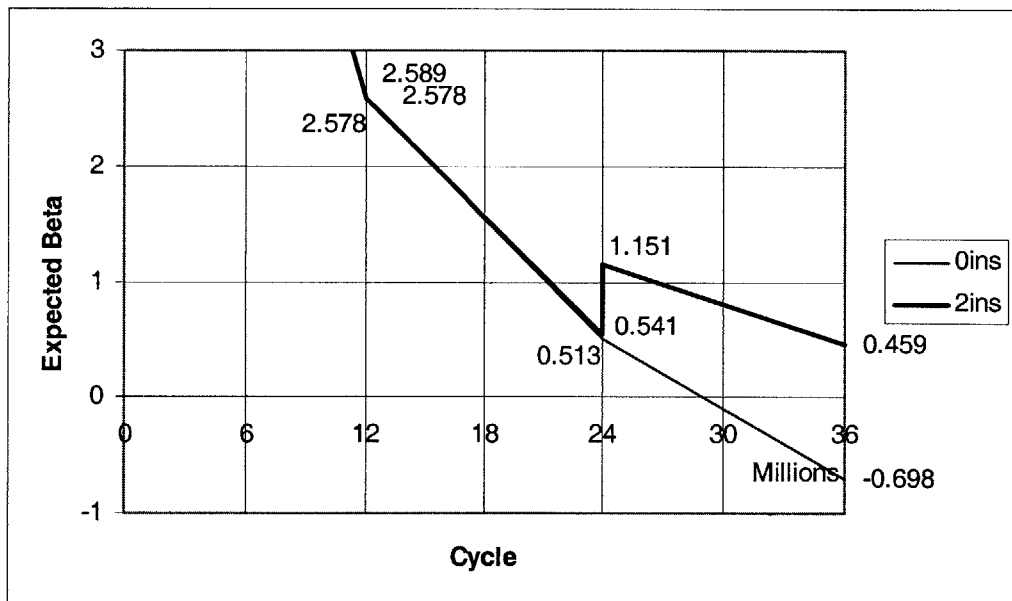
Fig. 3.15 Case of Two Inspections

69
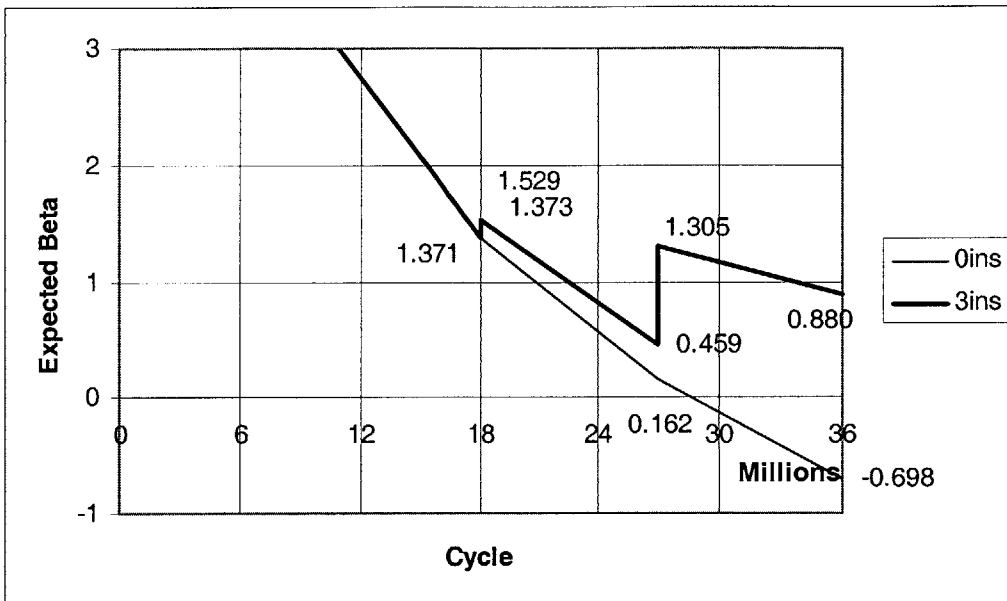
Fig. 3.16 Case of Three Inspections
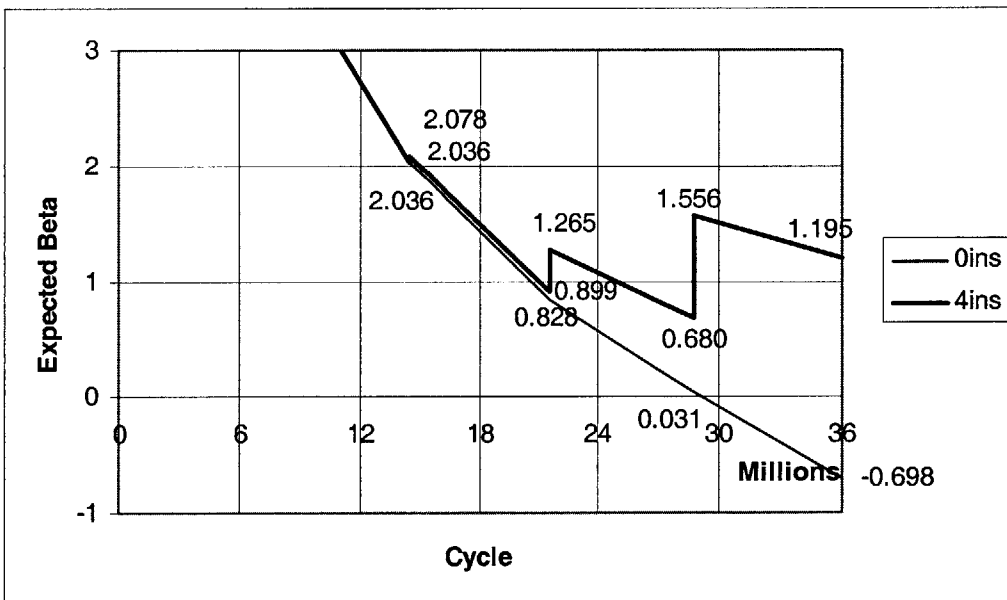
Fig. 3.17 Case of Four Inspections

70
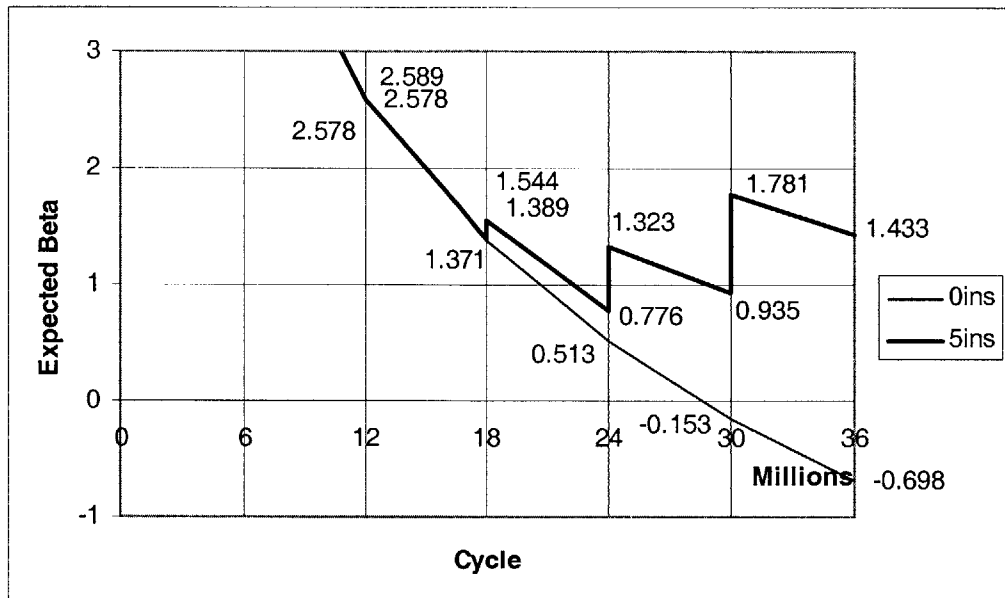
Fig. 3.18 Case of Five Inspections

3.5 LCC Analysis

3.5.1 LCC Model

An LCC analysis provides an economical evaluation of all current and future costs associated with investment alternatives. It is a valuable economic analytical technique for evaluating projects which require long-term capital and maintenance expenditure over the analytical period of infrastructures, such as bridges, dams, and railroads.

It is important to note that the same service life of each alternative must be used to yield valid results when implementing the LCC analysis. DOT (2002) refers to this

71

analytical service life, called analysis period as follows:

"LCC analysis uses a common period of time to assess cost difference between alternatives so that the results can be fairly compared. This time period is termed the analysis period. Allowing analysis period to vary among alternatives would result in the comparison of alternatives with different total cost, which is not appropriate under LCC analysis."

JR East sets up rules stipulating that the life of rails is 400 MGT (40 million stress cycles) based on Miner's law and engineering judgement. Additionally, many rails are replaced before reaching the critical number of load cycle because of the damage. Therefore, 360 MGT, a 90% of the value, is employed as the analysis period.

LCC analysis enables comparison of the costs of alternatives regarding inspection interval. The idea behind the LCC analysis is that decision related to inspection/repair intervention should consider all the costs imposed to the railroad companies incurred during the period over which the alternatives being compared. The costs regarding rail maintenance should consist of inspection and repair costs as well as costs due to the risk of a rail broken accident. Using an economic technique known as discounting, these costs are converted into the present value in the LCC analysis.

Inspection costs are those involved in regular inspection of rails. For a strategy involving n lifetime inspections, the total inspection cost, C_{INS} is expressed as

$$C_{INS} = \sum_{i=1}^{n} \frac{C_{ins}}{(1+r)^{t_i}} \qquad (3.44)$$

where, C_{ins} is each inspection cost based on the inspection technique, t_i is a time of inspection at i, and r is the discount rate.

Repair costs are those for the main structural work and include all the costs of structural assessment usually associated with repair decision-making. Rail repair costs, C_{rep} can be divided into

$$C_{rep} = C_{repa} + C_{repr} \qquad (3.45)$$

where, C_{repa} is the structural assessment costs including all the costs, such as contract cost with repair firms and re-investigation costs to identify the precise location, and C_{repr} is the structural repair costs include all the costs of the labor, material, equipment, administration to ensure safety under construction, and quality control. The ET is used to investigate all possible events related to repair or no-repair actions. It is recognized that a decision to either repair or no-repair needs to be made after every inspection to establish the ET. A repair decision made after every new inspection is influenced by decisions made in the past decision. Therefore, total repair cost should be expressed as a probabilistic expected value. The costs of repair associated with each branch, b_i are:

$$C_{rep,b_i} = \sum_{j=1}^{n} \frac{C_{rep}}{(1+r)^{t_j}} \qquad (3.46)$$

where, C_{rep,b_i} is the costs of repair associated with the branch, b_i and t_j is the time of repair. Therefore, the total expected repair cost, C_{REP} is expressed as

73

$$C_{REP} = \sum_{i=1}^{2^n} C_{rep,b_i} \cdot p_{bi} \qquad (3.47)$$

where, p_{b_i} is the probability of taken branch, b_i.

Failure cost, derived from the risk of rail broken accident, includes all the costs resulting from a broken rail. The total failure cost is defined as a product of the cost regarding failure and lifetime probability of failure calculated by FORM. The lifetime probability of failure is defined as

$$p_{f,life,b_i} = \max\left(p_{f,t_i,b_i}\right)$$
$$p_{f,life} = \sum_{i=1}^{2^n} p_{f,life,b_i} \cdot p_{b_i} \qquad (3.48)$$

where, $p_{f,life,b_i}$ is the probability of failure at branch, b_i $p_{f,life}$ is the lifetime probability of failure, and n is the number of inspection during the service life. Therefore, the total expected failure cost is expressed as

$$C_{FAIL} = C_f \cdot p_{f,life} \qquad (3.49)$$

where, C_{FAIL} is the total expected repair cost and C_f is failure cost.

The LCC is formulated by summating all the expected costs and expressed as

$$LCC = C_{INS} + C_{REP} + C_{FAIL} \qquad (3.50)$$

It is assumed that costs associated with failure, C_f are time-invariant to simplify the analysis. Allowances are not made for the derailment due to a broken rail, since the track safety system is remarkably redundant. The track signal system makes use of rails. If a rail break, the signal always changes to red, which means no train can get into the broken area. Even though a rail breaks just under a train, it turns out that the train

74

is able to pass safely as long as the gap due to the break is up to 70 [mm] from the in-depth experiment. Therefore, the probability of derailment is extremely small and negligible.

3.5.2 Parameters of LCC Analysis in Defect Management

A parametric study is carried out in order to investigate relative influences of main parameters on the total costs. For each parameter, a nominal value is selected. Table3.3 summarizes nominal values applied to the study. As alluded to the previous section, failure cost does not include derailment cost. It can be defined as the sum of repair cost and delay cost which indicates railroad companies pay back to passengers as a penalty based on covenant, if a train delays.

JR East pays back to passengers only when a train arrives late for the original timetable more than two hours at the destination. If a rail break, it is hard to replace it within two hours, so the repay cost can be failure cost in this study.

Table3.3 Nominal value of the Parameters in LCC Analysis

Cost	Notation	Nominal Value
Inspection Cost	C_{ins}	1
Structural Assessment Cost	C_{repa}	12.5
Structural Repair Cost	C_{repr}	37.5
Failure Cost	C_f	150

3.6 Summary

This chapter describes a methodology for optimization of rail inspection, reflecting the unique characteristics of rail defects such as trainload, crack growth rate, and the uncertainty of remedial actions. The following is a summary of the results obtained from the four analytical methods of LEFM, FORM, ET, and LCC.

- It turns out that the stress amplitude in rail bases is 50 [MPa] when train speed is 100 [km/h], wheel load is 10 [t], and 50N type rail, a conventional rail type in JR East. To simulate the stress amplitude, a continuously supported elastic model and a superposition method are employed.

- The stress that occurs at rail bases applied by trainload can be expressed by linear summation of static and dynamic stress. If both static and dynamic follow the stationary Gaussian random process, the stress amplitude follows Rayleigh distribution. Hence, the stress by trainload requires a probabilistic model.

- The rail resistance against trainload is considered as time-variant due to deterioration process. Rail base crack growth is recognized as a common cause of the deterioration. The prediction of crack growth in rail base at arbitrary times is evaluated by the semi-elliptical crack model based on Paris and Erdogan's law.

- FORM, a probabilistic method, is an adequate tool for assessing the structural safety and serviceability in order to take into account uncertainties associated with the prediction of crack growth, i.e., initial crack size and material parameters, as well as associated with the evaluation of reliability, i.e., critical crack size.

- FORM, one of the probabilistic approaches using first-order second moment approximation, is applicable for time-varying rail reliability because the results of FORM are always within 95% confidence interval, comparing the results by the Monte Carlo simulation with two million simulation samples.

- The ET can represent systematically all possible actions with respect to rail management, detection of defects, no-detection of defects, repair of the defects, and no-repair of the defects.

- The ET analysis is conducted considering both the uncertainty of NDT due to its imperfection, and remedial actions resulting from the decision-making process by solving other FORM regarding detecting defects and repairing defects.

- The LCC analysis model for rail management is formulated by summation of expected inspection cost, expected repair cost, and expected failure cost, taking into consideration the time value of money.

Chapter 4

Application and Results

4.1 Introduction

The purpose of this chapter is to postulate the optimal number of rail inspections in the first grade track of JR East, where more than two million trainload cycles a year occur by minimizing the expected total cost, the LCC including the expected inspection cost, the expected repair cost, and the expected failure cost.

In addition, this chapter presents the three results of sensitivity analysis. Since NDT is not perfect, as mentioned earlier, it is worthwhile to analyze the effect of other NDT techniques on the optimal number of rail inspections. Moreover, it is interesting how the optimal number of rail inspections changes when JR East alters the remedial action codes because the maintenance cost is related to frequency of inspection.

79

Furthermore, since it is arduous for railroad companies to evaluate accurate failure cost, it is advantageous to do sensitivity analysis for failure cost in LCC analysis.

4.2 Optimization of the Number of Inspections

4.2.1 Estimation of the LCC

As formulated in the previous chapter, the ET analysis can provide systematically all possible events regarding rail management. However, since the number of branches in the ET exponentially increases as the number of rail inspections increases, it is laborious to analyze the ET when the number of rail inspections is more than six or seven. For instance, when the number of rail inspections is 10, the number of branches in an ET becomes 3^{10}=59,049 and an ET has 3^{15}= 14,348,907 branches corresponding to 15 inspections. Therefore, some approximation methods are needed in order to assess the each expected cost instead of the ET analysis. Two million trainload cycles a year are employed in the analysis to compare with the actual JR East inspection codes. Discount rate is assumed to be 2%.

Fig. 4.1 shows the relationship between the expected inspection cost and the number of inspections. A linear relation is so conceivable that the linear trend line calculated by the least squares estimation method accordingly represents the relation as follows:

$$C_{INS} = 0.8406n - 0.0044 \qquad\qquad (4.1)$$

where, n is the number of inspections. Since the coefficient of determination, R is 1.0, the linear equation is perfectly exact to represent the relation. Fig. 4.2 depicts the relationship between the expected repair cost and the number of inspections. The expected cost gradually increases when the number of inspections increases so that a logarithm curve may be appropriate for the expression. The curve is obtained by the least squares estimation method as follows:

$$C_{REP} = 17.105\ln n + 11.238 \qquad\qquad (4.2)$$

R of this approximation is 0.998. It is general that the forecasting line is pertinent when the coefficient of determination is greater than 0.95. The logarithm curve is suitable for the arrangement. Fig. 4.3 exhibits the relationship between the expected failure cost and the number of inspections. Conceivably, the relation follows exponential estimation. The least squares estimator is similarly the best line to represent the relation as follows:

$$C_{FAIL} = 97.583\exp[-0.1357n] \qquad\qquad (4.3)$$

R is 0.992 in this approximation.

As a result, the LCC is formulated by the following equation, which is a function of the inspection number.

$$\begin{aligned} LCC &= 0.8406n - 0.0044 + 17.105\ln n + 11.238 + 97.583\exp[-1.357n] \\ &= 0.846n + 17.105\ln n + 97.583\exp[-1.357n] + 11.2336 \end{aligned}$$

$$\qquad\qquad (4.4)$$
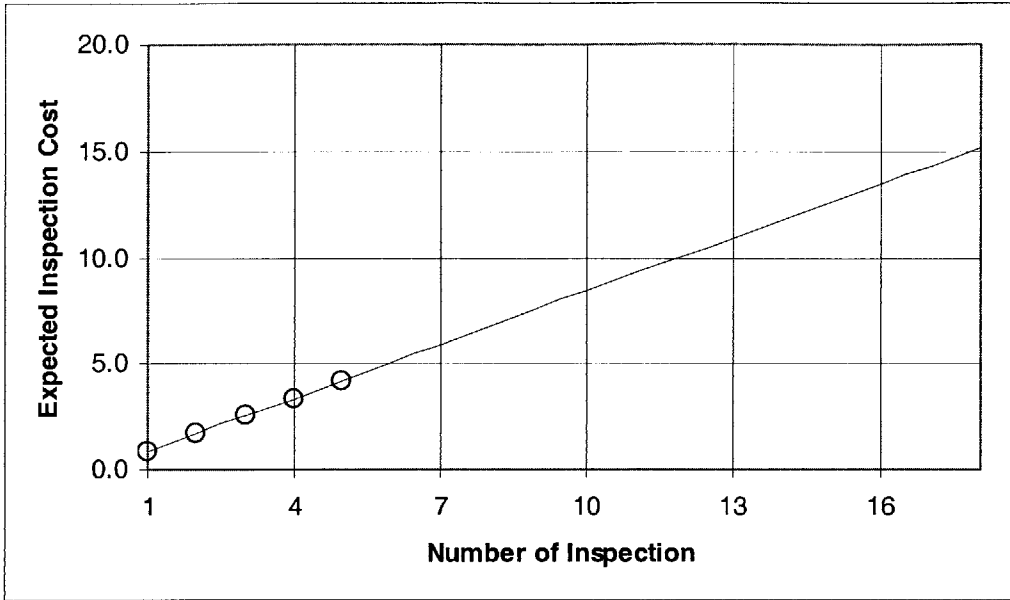
Fig. 4.1 Relationship between the Expected Inspection Cost and the Number of Inspections
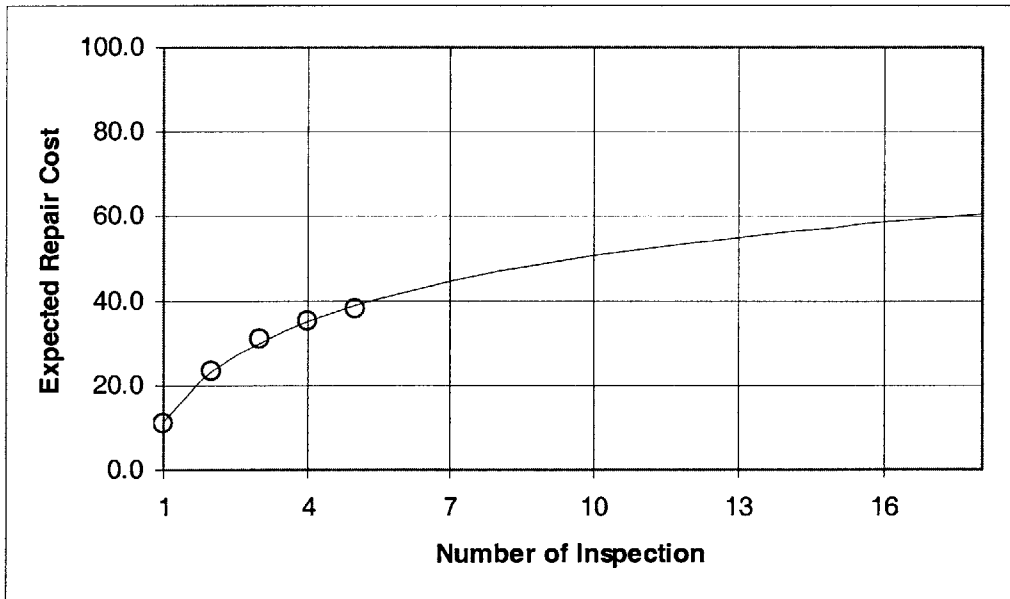
Fig. 4.2 Relationship between the Expected Repair Cost and the Number of Inspections
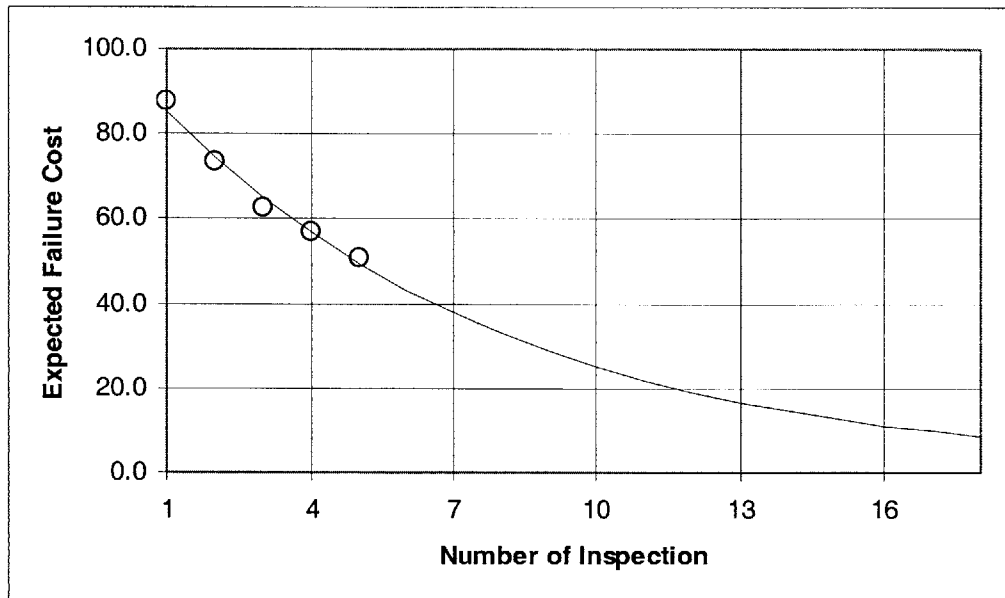
Fig. 4.3 Relationship between the Expected Failure Cost and the Number of Inspections

4.2.2 The Optimal Number of Rail Inspections

Table4.1 and Fig. 4.4 show the results of the analysis for the different number of rail inspections in the LCC, using the approximation method mentioned in the previous section. It is interesting to note that the expected costs for inspection and repair increase whereas the expected failure cost decreases, as the number of inspection increases. This indicates that the increment of the inspection can improve the reliability of rails. In this manner, there is a trade-off point at which the LCC is minimized. From Fig. 4.4, it is found that an optimal number of rail inspections are 14 and the minimum LCC is 82.741, in other word; rail inspection should be done every 2.57 million trainload cycles.

Table4.1 Results of LCC Analysis

Number of Inspection	C_{INS}	C_{REP}	C_{FAIL}	LCC
1	0.836	11.238	85.200	97.274
2	1.677	23.094	74.389	99.160
3	2.517	30.030	64.949	97.496
4	3.358	34.951	56.707	95.016
5	4.199	38.767	49.511	92.477
6	5.039	41.886	43.229	90.154
7	5.880	44.523	37.743	88.146
8	6.720	46.807	32.954	86.481
9	7.561	48.822	28.772	85.155
10	8.402	50.624	25.121	84.146
11	9.242	52.254	21.933	83.429
12	10.083	53.742	19.150	82.975
13	10.923	55.111	16.720	82.755
14	11.764	56.379	14.598	82.741
15	12.605	57.559	12.746	82.910
16	13.445	58.663	11.128	83.237
17	14.286	59.700	9.716	83.702
18	15.126	60.678	8.483	84.288
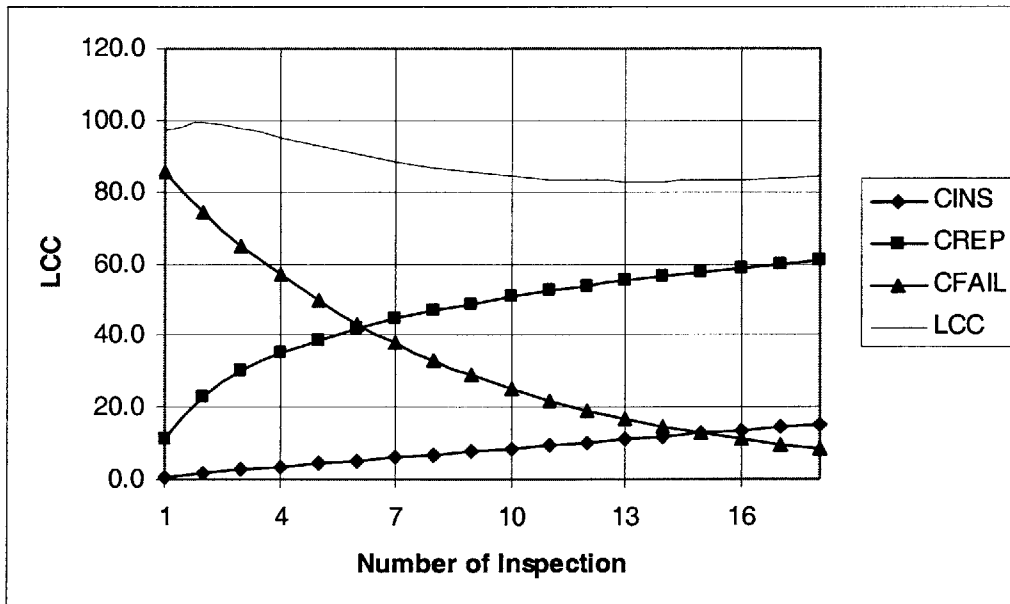
Fig. 4.4 Results of LCC Analysis

4.2.3 Discussions

The following lists results and suggestions obtained from the LCC analysis with new estimation model with respect to the expected costs.

- It turns out that a statistical approximation method can express the relationship between the expected cost and the number of inspections regarding rail defect management, avoiding the laborious calculation of the ET analysis.

- As mentioned earlier, JR East requires the track engineers to inspect rails every two million wheel load cycles. As there are about two million wheel load cycles a year in the first grade tracks, the engineers have to test the rails by NDT once a year. It is possible to extend this inspection interval from 20.0MGT into 25.7MGT on the basis of the results of this research. However, other defects including rail head and bolt-hole cracks should be considered for the final decision about inspection interval extension.

4.3 Sensitivity Analysis

4.3.1 The Effect of NDT Techniques

There are several types of NDT techniques, such as sliding and rolling probes in the ultrasonic inspection technique. Generally speaking, the more expensive NDT

technique is, the more capable the technique is. Hence, the types of NDT techniques have a significant effect on the optimal number of rail inspections. Three different inspection devices are used to illustrate the effect in the study. The detectability, accuracy, and cost associated with each NDT technique are shown in Table4.2 and Fig. 4.5. All the PODs are assumed to follow lognormal distribution. It is clear that type A is most detactable and accurate among them while type C is the least one.

In addition to the above sensitivity analysis, the simulation of LCC is conducted for the effect of both detecability and accuracy of NDT. Table4.3, Fig.4.6, and Fig4.7 show the cases for the simulation. All the costs of NDT are identical for the comparison. $C_{ins} = 1.0$ and $C_{ins} = 0.5$ are used for the simulation. Although NDT of case D, E, and F have the same accuracy, they have different detectability. On the other hand, NDT of case D, G, and H have the same detectability and different accuracy.

Table 4.2 Condition of Sensitivity Analysis for POD

Technique	Type	Detectability	Accuracy	Cost
A	lognormal	0.5	0.05	1
B	lognormal	1.0	0.05	0.5
C	lognormal	2.0	0.2	0.25

Table4.3 Condition of Sensitivity Analysis for Detectability and Accuracy

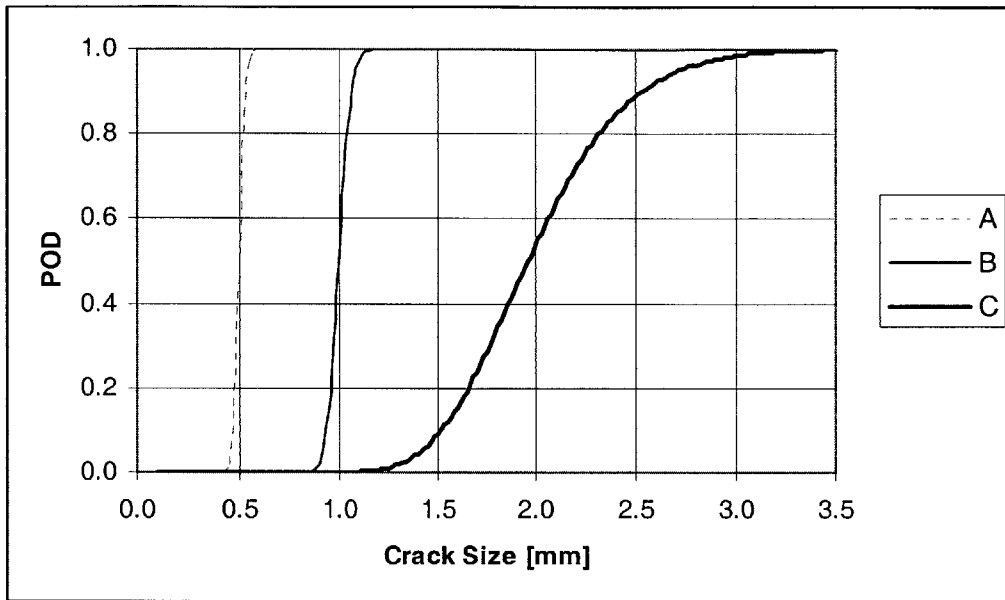| Case	Type	Detectability	Accuracy
D	lognormal	1.0	0.05
E	lognormal	2.0	0.05
F	lognormal	3.0	0.05
G	lognormal	1.0	0.25
H	lognormal	1.0	0.5

Fig. 4.5 Capability of Inspection for Sensitivity Analysis
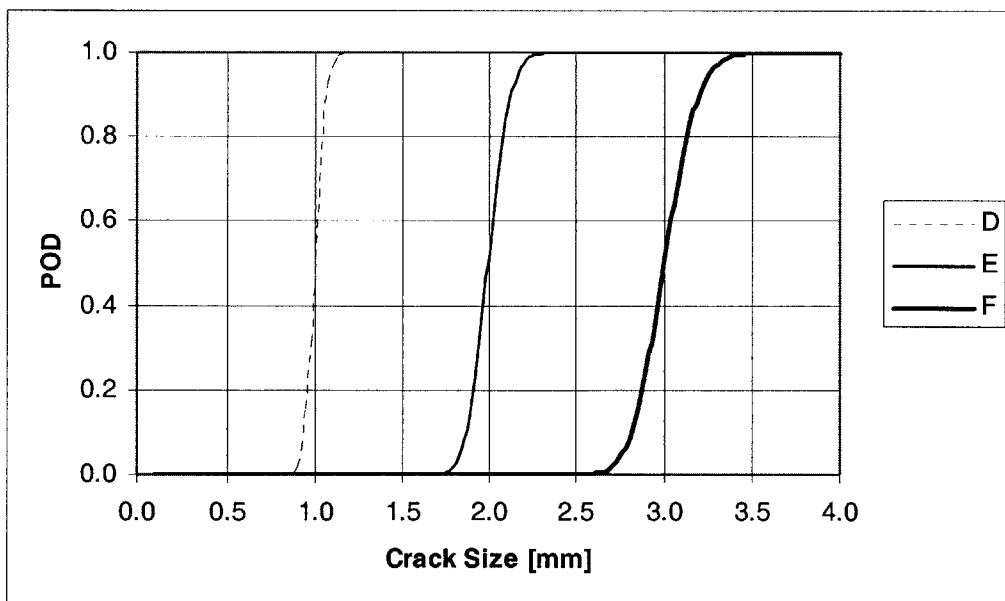

Fig. 4.6 Capability of Inspection for Sensitivity Analysis of Detectability
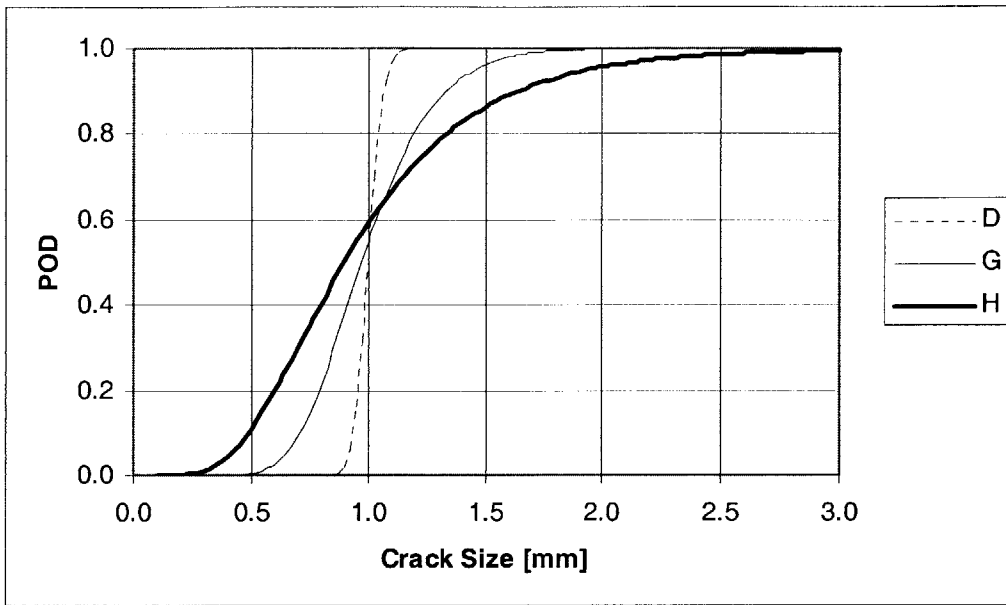
Fig. 4.7 Capability of Inspection for Sensitivity Analysis of Accuracy
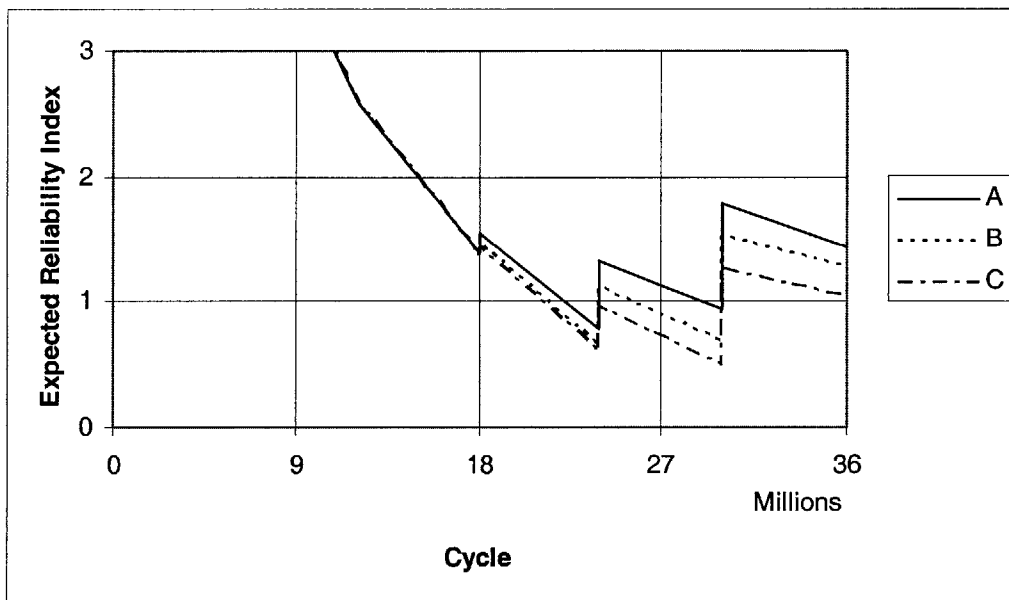
Fig. 4.8 Relationship between the Expected Reliability Index and Trainload

Cycle in Sensitivity Analysis for POD

Fig. 4.8 shows the expected reliability index in NDT technique type A, B, and C, when the number of rail inspection is five. As expected, the more detective and accurate inspection device is, the more the expected reliability index is improved. Fig. 4.9 shows the relationship between the expected repair cost and the number of inspection in NDT technique type B and C (Type A is already investigated in the section 4.2). The approximation line is obtained from this results as follows

$$C_{REP(B)} = 18.01 \ln n + 6.6014 \qquad (4.5)$$

$$C_{REP(C)} = 17.156 \ln n + 3.8099 \qquad (4.6)$$

R of equation (4.5) and (4.6) is 0.999. Fig. 4.10 depicts the relationship between the expected failure cost and the number of inspections. Similarly above, the least squares estimator is:

$$C_{FAIL(B)} = 105.97 \exp[-0.098n] \qquad (4.7)$$

$$C_{FAIL(C)} = 110.09 \exp[-0.1186n] \qquad (4.8)$$

R of equation (4.7) and (4.8) is 0.981. Tabale4.4 and Table4.5 corresponding to Fig. 4.11 and Fig. 4.12 show the results of LCC analysis for NDT technique type B and C respectively based on the above approximation method.

It can be seen that the LCC decreases when the inspection cost is half of the original one, even though the detectability of NDT deteriorates from 0.5 [mm] into 1.0 [mm]. Similar conclusion can be drawn from Tabale4.5. The LCC with respect to the low capable NDT is smaller than that of high performance NDT, if the cost is one-fourth original one.

89
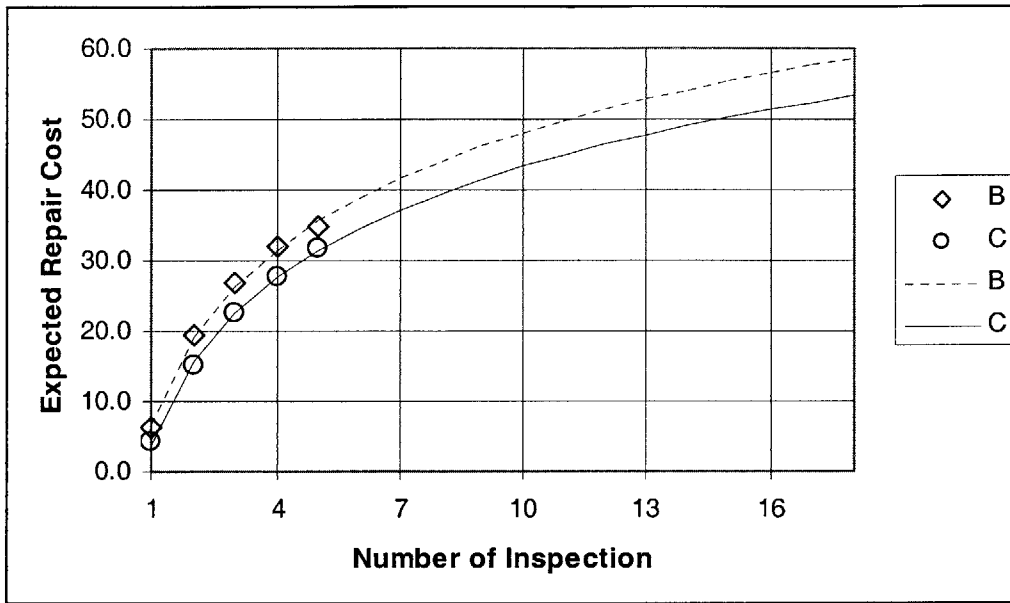
Fig. 4.9 Relationship between Expected Repair Cost and the Number of Inspections in Sensitivity Analysis for POD
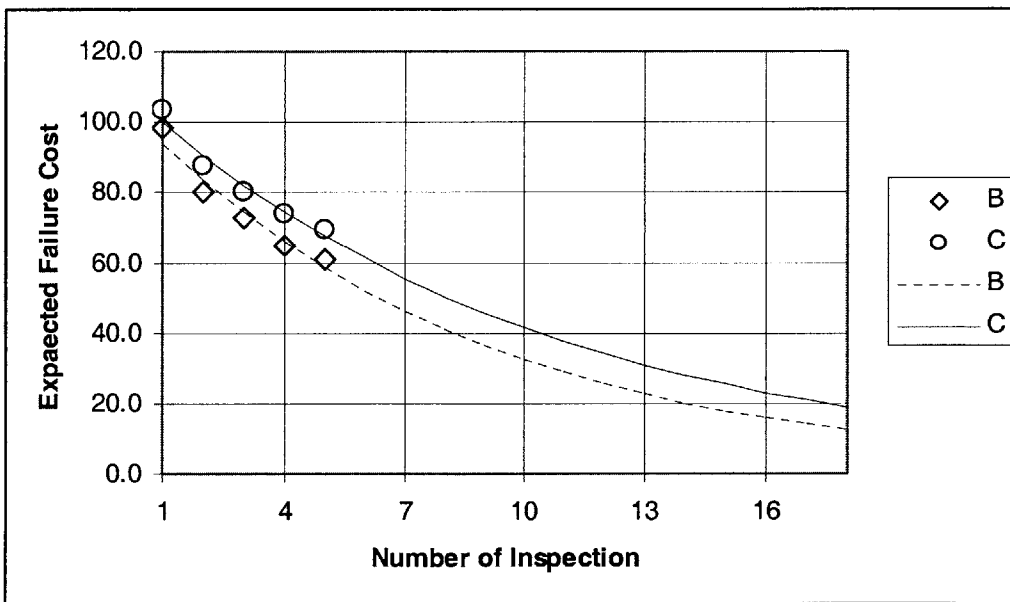
Fig. 4.10 Relationship between Expected Repair Cost and the Number of Inspections in Sensitivity Analysis for POD

Table4.4 Results of LCC Analysis in Type B NDT

Number of Inspection	C_{INS}	C_{REP}	C_{FAIL}	LCC
1	0.418	6.601	94.119	101.138
2	0.838	19.085	83.593	103.516
3	1.258	26.387	74.244	101.890
4	1.679	31.569	65.941	99.188
5	2.099	35.587	58.566	96.252
6	2.519	38.871	52.016	93.407
7	2.940	41.647	46.199	90.786
8	3.360	44.052	41.032	88.444
9	3.780	46.173	36.443	86.397
10	4.201	48.071	32.368	84.639
11	4.621	49.787	28.748	83.156
12	5.041	51.355	25.533	81.928
13	5.461	52.796	22.677	80.935
14	5.882	54.131	20.141	80.153
15	6.302	55.373	17.888	79.564
16	6.722	56.536	15.888	79.146
17	7.143	57.628	14.111	78.881
18	7.563	58.657	12.533	78.753
19	7.983	59.631	11.131	78.745
20	8.404	60.555	9.886	78.844
21	8.824	61.433	8.781	79.038
22	9.244	62.271	7.799	79.314
23	9.664	63.072	6.927	79.663
24	10.085	63.838	6.152	80.075
25	10.505	64.573	5.464	80.542
26	10.925	65.280	4.853	81.058
27	11.346	65.959	4.310	81.615
28	11.766	66.614	3.828	82.208
29	12.186	67.246	3.400	82.833
30	12.607	67.857	3.020	83.483
31	13.027	68.448	2.682	84.156
32	13.447	69.019	2.382	84.848
33	13.867	69.574	2.116	85.557
34	14.288	70.111	1.879	86.278
35	14.708	70.633	1.669	87.010
36	15.128	71.141	1.482	87.751

Table4.4 Results of LCC Analysis in Type C NDT

| Number of Inspection	C_{INS}	C_{REP}	C_{FAIL}	LCC
1	0.084	3.810	99.813	103.707
2	0.168	15.702	90.495	106.365
3	0.252	22.658	82.047	104.957
4	0.336	27.593	74.388	102.317
5	0.420	31.421	67.444	99.285
6	0.504	34.549	61.148	96.201
7	0.588	37.194	55.440	93.222
8	0.672	39.485	50.264	90.421
9	0.756	41.505	45.572	87.834
10	0.840	43.313	41.318	85.471
11	0.924	44.948	37.461	83.333
12	1.008	46.441	33.964	81.413
13	1.092	47.814	30.793	79.700
14	1.176	49.086	27.919	78.180
15	1.260	50.269	25.312	76.842
16	1.344	51.376	22.950	75.670
17	1.428	52.417	20.807	74.652
18	1.512	53.397	18.865	73.774
19	1.596	54.325	17.104	73.024
20	1.680	55.205	15.507	72.392
21	1.764	56.042	14.059	71.865
22	1.848	56.840	12.747	71.435
23	1.932	57.602	11.557	71.092
24	2.016	58.333	10.478	70.827
25	2.100	59.033	9.500	70.633
26	2.184	59.706	8.613	70.503
27	2.268	60.353	7.809	70.430
28	2.352	60.977	7.080	70.409
29	2.436	61.579	6.419	70.434
30	2.520	62.161	5.820	70.501
31	2.604	62.723	5.277	70.604
32	2.688	63.268	4.784	70.740
33	2.772	63.796	4.338	70.905
34	2.856	64.308	3.933	71.097
35	2.940	64.805	3.565	71.311
36	3.024	65.289	3.233	71.545
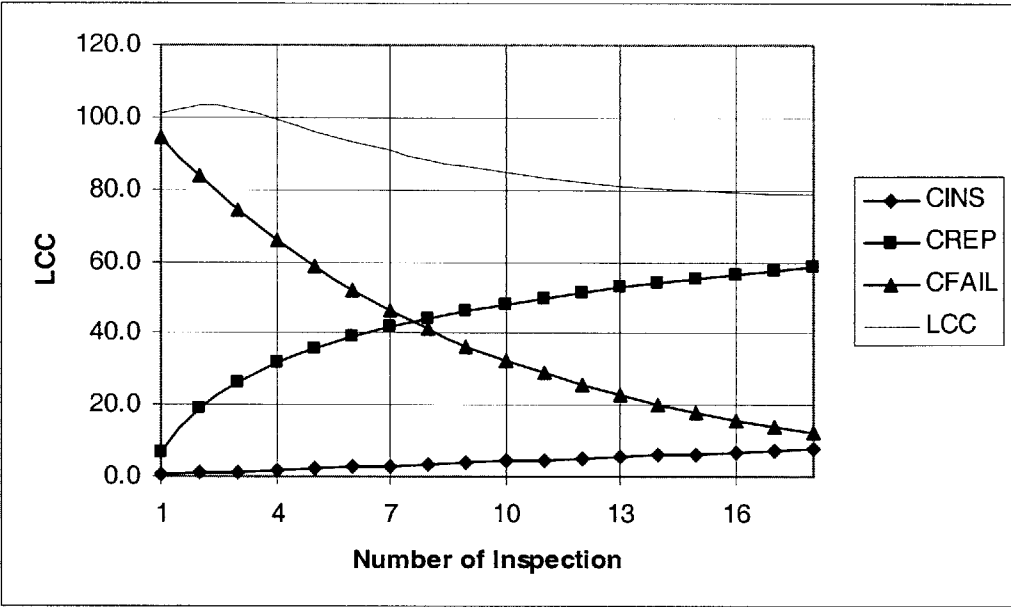
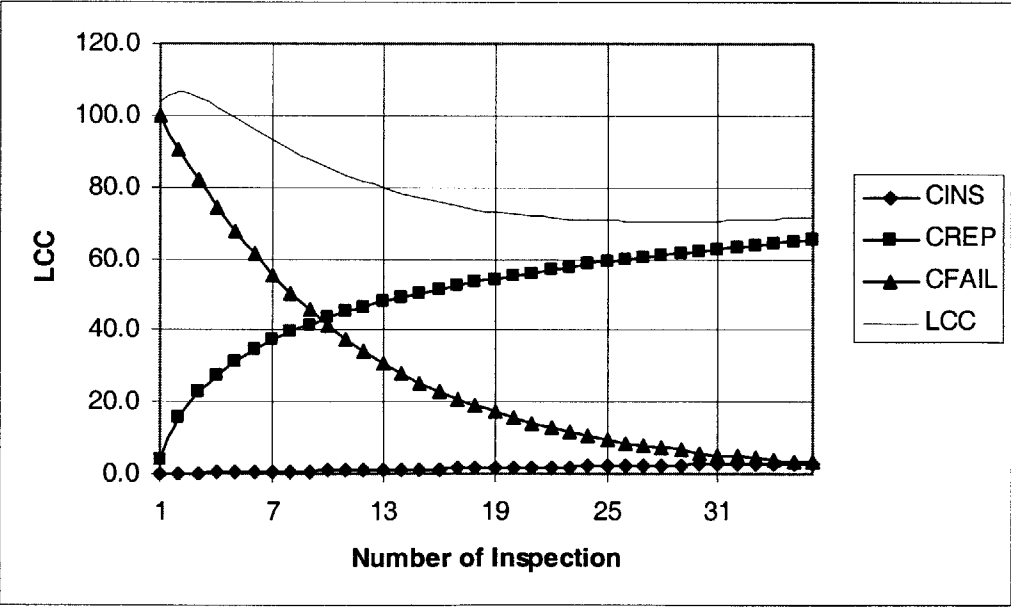**Fig. 4.11 Result of LCC Analysis in Type B NDT**

Fig. 4.12 Result of LCC Analysis in Type C NDT
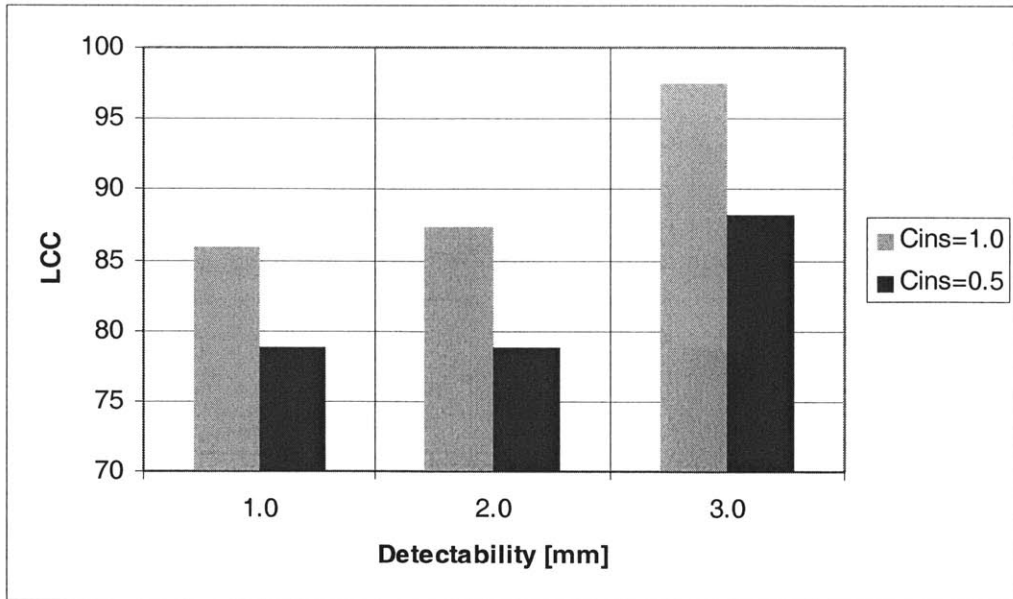
Fig. 4.13 Relationship between the LCC and Detectability of NDT
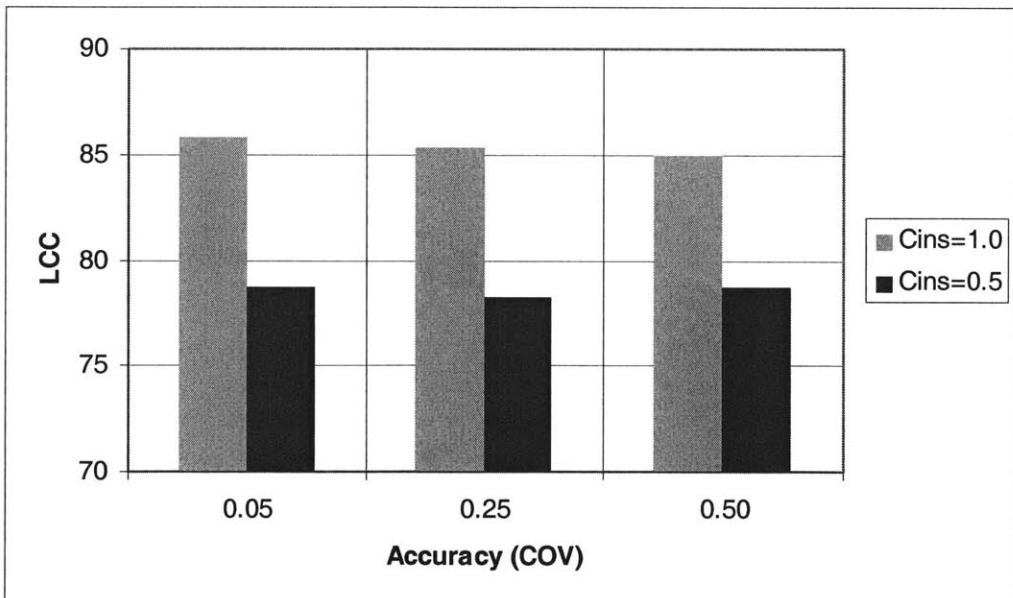

Fig. 4.14 Relationship between the LCC and Accuracy of NDT

Fig. 4.13 shows the relationship between the LCC and the different detectable NDT techniques. Fig. 4.14 displays the relationship between the LCC and the different accurate NDT techniques. It can be seen that the LCC is not sensitive to accuracy of NDT but sensitive to their detectability. If the low performance NDT is developed at half a cost of original one, the LCC is the same as medium performance NDT.

4.3.2 The Effect of Repair Regulation

This study considers three POR approaches, which indicate that JR East tightens remedial action codes and loosens the codes. JR East spends 30% of the operational cost for the maintenance, as alluded to chapter 1. It is beneficial to analyze the effect of changing the remedial action codes on the optimal number of rail inspections, because modification of remedial action codes may reduce the total maintenance cost. Fig. 4.15 shows the three PORs when a_r is 1.5 [mm], 2.0 [mm], and 2.5 [mm], respectively. As summarized in Tabale1.1, JR East requires the track engineers to repair immediately rails when they find more than 3.0 [mm] cracks in the rails. Since the POR is modeled to describe this policy in this thesis, the change of a_r from 2.0 [mm] into 1.5 [mm] indicates that the track engineers must take immediately a remedial action if they detect a crack of the more than 2.0 [mm]. Similarly, when a_r is 2.5 [mm], the engineers have to repair immediately the rail that has a crack of more than 4.0 [mm]. All PORs are assumed to be uniformly distributed. Table4.6 summarizes the condition of this sensitivity analysis.

Fig. 4.16 displays the expected reliability index in five inspections during the service life. As expected, the expected reliability index is smaller than that of the original code, when the remedial action code is loosen. Fig. 4.17 shows the relationship between the expected repair cost and the number of inspections in type a and c (Type b is already analyzed in the section 4.2). As a result, the approximation line is obtained from the outputs as follows:

$$C_{REP(a)} = 16.684 \ln n + 13.95 \qquad (4.9)$$

$$C_{REP(c)} = 17.28 \ln n + 9.5141 \qquad (4.10)$$

R in type a is 0.996 and R in type c is 0.999. Fig. 4.18 shows the relationship between the expected failure cost and the number of inspections. Similarly the trend lines are:

$$C_{FAIL(a)} = 92.598 \exp[-0.148n] \qquad (4.11)$$

$$C_{FAIL(c)} = 100.72 \exp[-0.1284n] \qquad (4.12)$$

R in type a is 0.992 and R in type c is 0.991. Table4.7 and 4.8 corresponding to Fig. 4.19 and Fig. 4.20 show the results for different numbers of inspections in the LCC analysis when a_r is 1.5 [mm] and 2.5 [mm], respectively.

Table 4.6 Condition of Sensitivity Analysis for POR

Case	Type	a_r	Definition
a	uniform	1.5	If crack size is more than 2 [mm], the rail must be replaced immediately
b	uniform	2.0	If crack size is more than 3 [mm], the rail must be replaced immediately
c	uniform	2.5	If crack size is more than 4 [mm], the rail must be replaced immediately
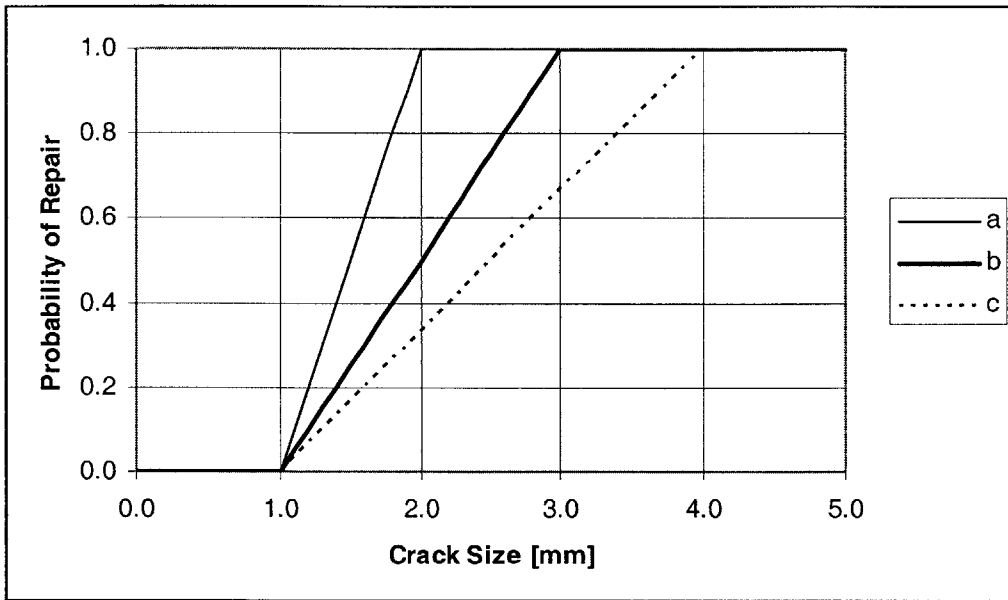
Fig. 4.15 Probability of Repair for Sensitivity Analysis
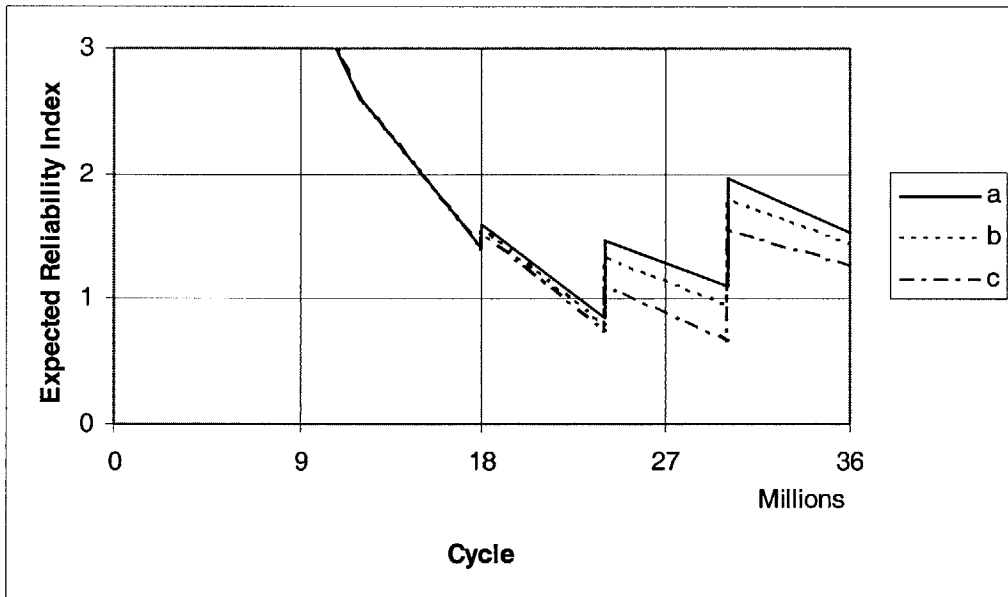
Fig. 4.16 Relationship between Expected Reliability Index and Trainload

Cycle in Sensitivity Analysis for Remedial Actions
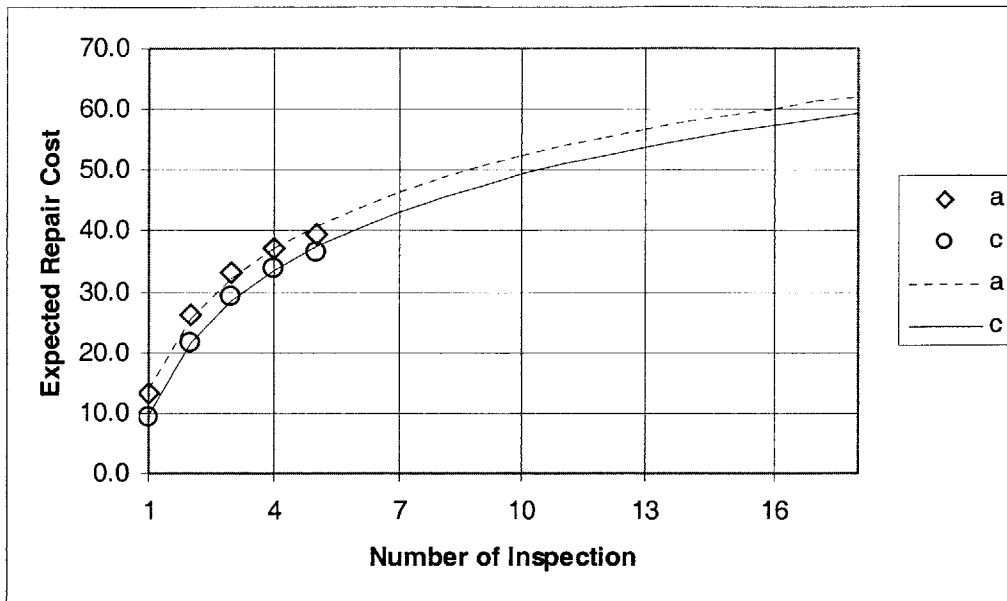
Fig. 4.17 Relationship between Expected Repair Cost and the Number of Inspections in Sensitivity Analysis for Remedial Actions
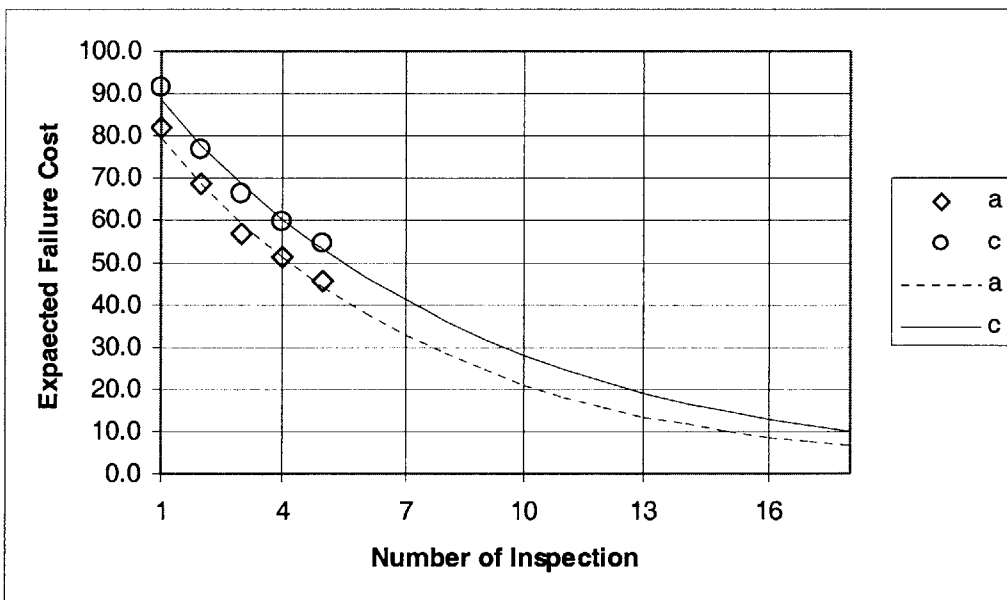
Fig. 4.18 Relationship between Expected Failure Cost and the Number of Inspections in Sensitivity Analysis for Remedial Actions

Table4.7 Results of LCC Analysis in a_r=1.5 [mm]

Number of Inspection	C_{INS}	C_{REP}	C_{FAIL}	LCC
1	0.836	13.950	79.851	94.638
2	1.677	25.514	68.859	96.051
3	2.517	32.279	59.381	94.177
4	3.358	37.079	51.207	91.643
5	4.199	40.802	44.158	89.158
6	5.039	43.844	38.079	86.962
7	5.880	46.416	32.837	85.133
8	6.720	48.643	28.317	83.681
9	7.561	50.608	24.419	82.589
10	8.402	52.366	21.058	81.826
11	9.242	53.956	18.159	81.358
12	10.083	55.408	15.659	81.150
13	10.923	56.744	13.504	81.171
14	11.764	57.980	11.645	81.389
15	12.605	59.131	10.042	81.778
16	13.445	60.208	8.660	82.313
17	14.286	61.219	7.468	82.973
18	15.126	62.173	6.440	83.739
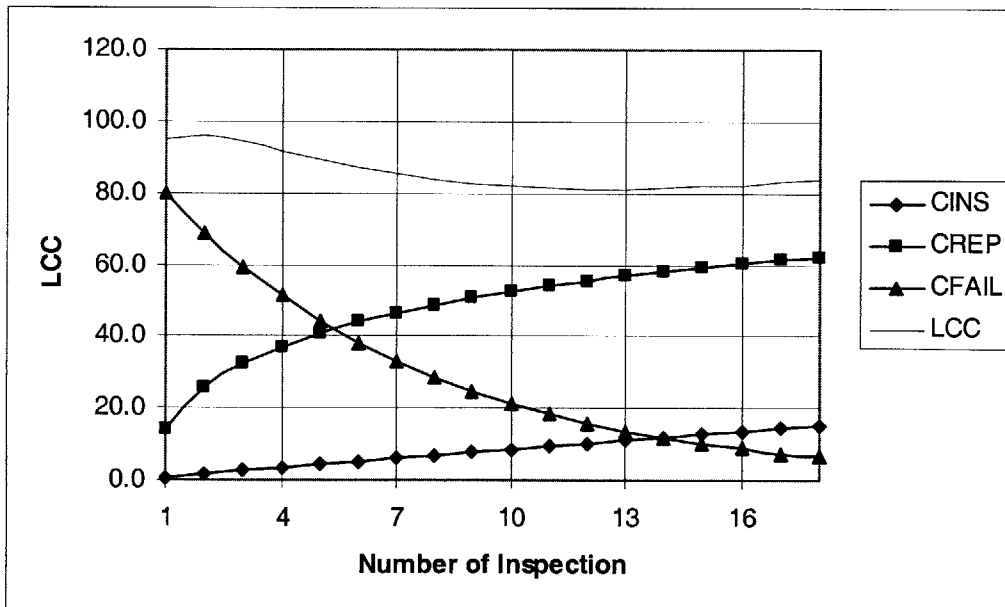
Fig. 4.19 Table4.6 Results of LCC Analysis in a_r=1.5 [mm]

Table4.8 Results of LCC Analysis in a_r=2.5 [mm]

Number of Inspection	C_{INS}	C_{REP}	C_{FAIL}	LCC
1	0.836	9.514	88.583	98.934
2	1.677	21.492	77.909	101.078
3	2.517	28.498	68.521	99.537
4	3.358	33.469	60.265	97.092
5	4.199	37.325	53.003	94.527
6	5.039	40.476	46.616	92.131
7	5.880	43.139	40.999	90.018
8	6.720	45.447	36.059	88.226
9	7.561	47.482	31.714	86.757
10	8.402	49.303	27.892	85.596
11	9.242	50.950	24.531	84.723
12	10.083	52.453	21.575	84.111
13	10.923	53.836	18.975	83.735
14	11.764	55.117	16.689	83.570
15	12.605	56.309	14.678	83.592
16	13.445	57.424	12.909	83.779
17	14.286	58.472	11.354	84.112
18	15.126	59.460	9.986	84.572
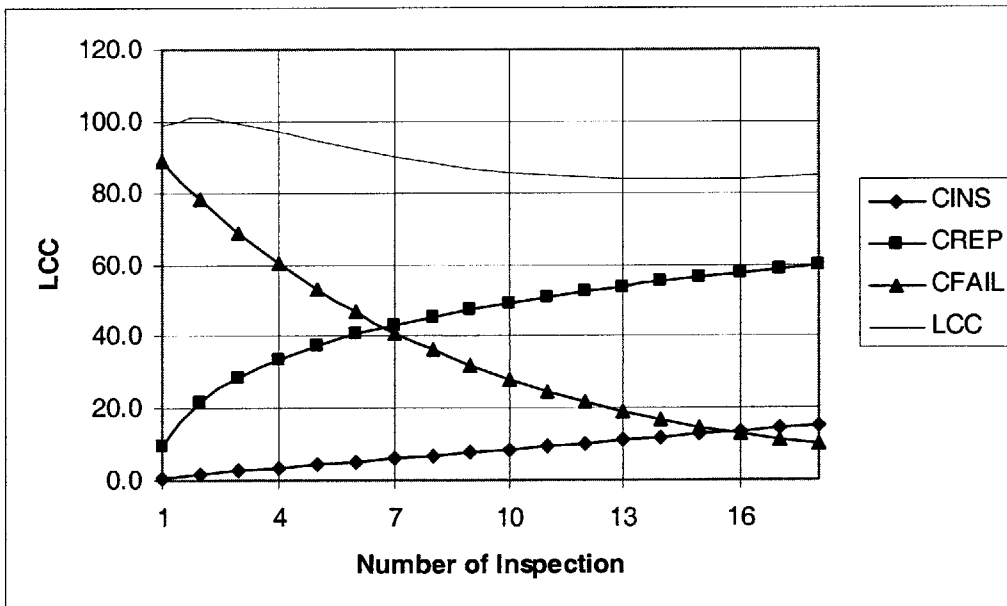
Fig. 4.20 Result of LCC Analysis in a_r=2.5 [mm]

It can be seen that the LCC is smaller than that of original code when a proactive maintenance policy is employed, which implies a tightened repair codes.

4.3.3 The Effect of Failure Cost

A LCC analysis is the one of the comprehensive economic means of comparing project investments and maintenance expenditures. The LCC analysis has applications in many interest areas for government and private infrastructure sectors, such as highways, ports, and railroads.

However, the LCC analysis has several controversial problems when providing outputs. The most significant of them is cost uncertainty. When data are collected to support the LCC analysis, there may be uncertainties in economic values of inputs and outputs. In particular, failure cost may represent the greatest challenging to the LCC analysis implementation, since the estimation is very intricate. Although the failure cost is assumed to be an invariant repay cost to passengers in this thesis, it fundamentally depends on the ride rate of each train. Failure cost can be random variables. Therefore, sensitivity analysis for failure cost is important for the decision process of rail defect management, instead of regarding the failure cost as random variables.

Fig. 4.21 shows the relationship between the failure cost and the optimal number of rail inspections, when failure cost varies from 150 to 500 in nominal values. Fig. 4.22 also shows the same relationship when using the optimal inspection interval instead of the optimal number of inspections.

101
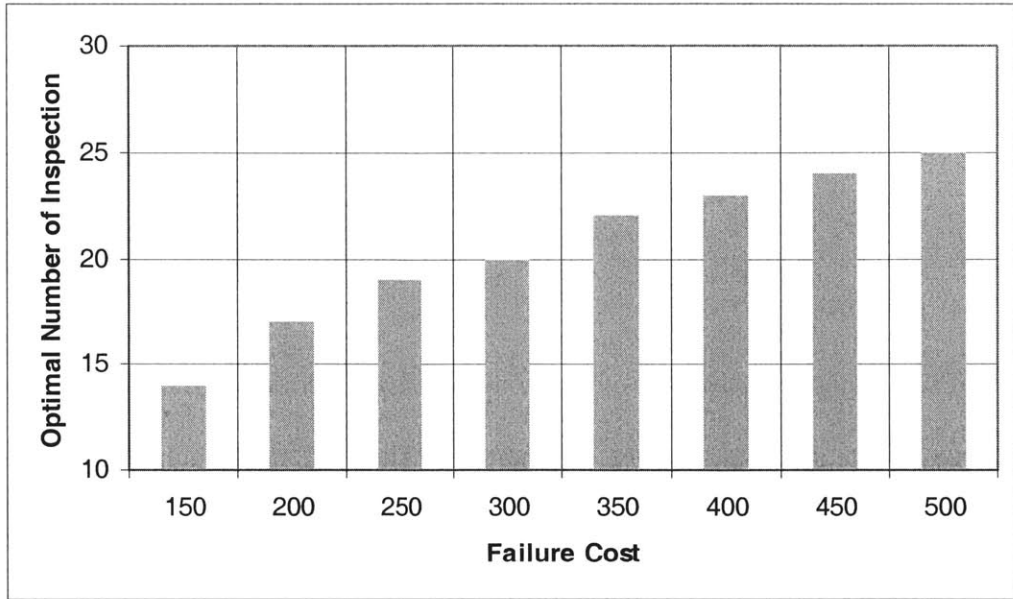
Fig. 4.21 Results of Sensitivity Analysis for Failure Cost
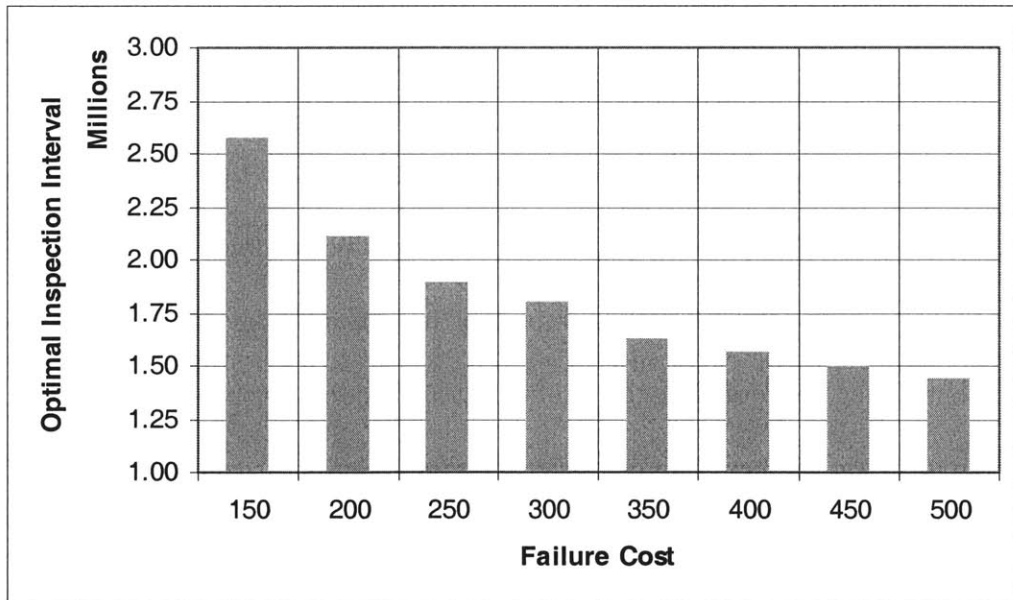
Fig. 4.22 Results of Sensitivity Analysis for Failure Cost

4.3.4 Discussions

For the purpose of evaluating the effect of parameters on the LCC analysis and the optimal number of inspections, sensitivity analysis is conducted. The important results and suggestions through sensitivity analysis are summarized in the following:

- It turns out that the detectability of NDT has greater influence on the LCC than the accuracy of NDT has on the LCC. This indicates that JR East should attempt to develop NDT devices with increasing high detectability, even if they have a few errors.

- Even if the remedial action policy is modified with an increase of LCC, the optimal number of inspection would be identical to that of original policy. However, a proactive maintenance policy, which implies a tightened repair code, can reduce both the LCC and the optimal number of inspections.

- The optimal number of inspections and the LCC are highly dependant on the failure costs. For instance, it can be seen that the optimal number of inspections increases by 1.7 times if the failure cost is three times the original cost. Therefore, decision-makers should make a judgement about the failure costs on the basis of calibrations when evaluating the optimal number of inspections.

The application of the presented model to the process of optimization of inspection/repair intervention represents a significant advance in the decision-making process with regard to rail defect management. Instead of basing decisions about inspection intervals on empirical judgement, the model presents a quantitative method for making these decisions, taking into consideration on uncertainties with respect to rail defects management. All results of sensitivity analysis are summarized in Table4.9.

Table4.9 Overall Summary of Sensitivity Analysis

POD		POR	Cost			Optimal Inspection Interval [Million]	LCC
Detectability	Accuracy (COV)	a_r	C_{ins}	C_{rep}	C_{fail}		
0.5	0.05	2.0	1.0	50	150	2.57	82.742
1.0	0.05	2.0	0.5	50	150	1.89	78.745
2.0	0.2	2.0	0.25	50	150	1.29	70.409
1.0	0.05	2.0	1.0	50	150	2.40	85.866
2.0	0.05	2.0	1.0	50	150	2.00	87.410
3.0	0.05	2.0	1.0	50	150	1.80	97.495
1.0	0.25	2.0	1.0	50	150	2.25	83.348
1.0	0.5	2.0	1.0	50	150	2.40	84.962
0.5	0.05	1.5	1.0	50	150	3.00	81.150
0.5	0.05	2.5	1.0	50	150	2.57	83.570
0.5	0.05	2.0	1.0	50	200	2.12	86.941
0.5	0.05	2.0	1.0	50	250	1.89	89.914
0.5	0.05	2.0	1.0	50	300	1.80	92.222
0.5	0.05	2.0	1.0	50	350	1.64	94.102
0.5	0.05	2.0	1.0	50	400	1.57	95.678
0.5	0.05	2.0	1.0	50	450	1.50	97.043
0.5	0.05	2.0	1.0	50	500	1.44	98.245

4.4 Summary

This chapter gives details of applications and results based on the methodology and outputs of the previous chapter. First of all, the optimal inspection interval is postulated. It is determined that the extension of inspection interval is possible. Next, the sensitivity of the optimal inspection interval for different NDT techniques is investigated. Results indicate that though the accuracy of NDT does not affect the LCC, the detectability of NDT is significant for the LCC. Moreover, the investigation of repair regulation indicates a proactive maintenance policy may reduce the LCC. Finally, some suggestions obtained from the applications are discussed.

Chapter 5

Conclusion

5.1 Summary

This thesis discusses some applications of the modeling work to rail defect management. In particular, two main applications are described as follows:

- Determination of the optimal inspection interval on the basis of the quantitative approach.

- Measurement of the effect of inspection equipment and of remedial actions on the optimal inspection interval and the LCC.

The frequency of rail inspections tends to vary from one railroad to another, yet it is usually based on either time or traffic tonnage. Railroad companies have evolved their rail inspection schedules empirically, based on long field experience. Rail defect

management refers to the development and implementation of strategies to control the risk of rail failure. The primary method to control the risk is a rail inspection through nondestructive evaluation and is a replacement of rails based on the evaluation results.

To demonstrate the feasibility of the above applications, first, a Linear Elastic Fracture Mechanics (LEFM) analysis which can predict a crack size in a rail base is performed. Second, a First-Order Reliability Methods (FORM) analysis evaluates the reliability of a rail, considering some uncertainties of parameters. Third, an Event Tree (ET) analysis represents systematically all possible events and actions regarding rail defect management. Finally, a Life-Cycle Cost (LCC) analysis formulates the total expected cost during the service life are conducted.

5.2 Conclusions

The main conclusions obtained from the research are:

- **At every 2.57 million trainload cycles, rail inspection should be done.**

Since the present inspection interval is two million trainload cycles in JR East, it is possible to extend the interval in order to reduce the total cost of rail defect management; when inspection cost 1, repair cost 50, and failure cost 150 in nominal value, analysis period 360MGT, wheel load 10 [t], train speed 100 [km/h], all uncertain parameters follow lognormal distribution.

108

- **Detectability of NDT is the significant parameter in the process of determining the optimal inspection interval.**

It turns out that the detectability of NDT has more influences on the LCC than does the accuracy of NDT. This indicates that JR East should attempt to develop devices of NDT of high detectability, even if they must sacrifice some accuracy.

- **A proactive maintenance policy reduces both the LCC and the number of inspections.**

In the present remedial action codes, JR East requires the track engineers to replace the any rails that include base crack of more than 3 [mm]. The alternation from 3 [mm] into 2 [mm] reduces the LCC and extend the inspection interval. JR East should adopt a proactive maintenance policy.

5.3 Recommendations for Future Work

This thesis demonstrates the feasibility of reliability-based optimization of rail inspection. However, several issues need further development and refinement, before the presented approach should be implemented into practice.

- **Combination with other types of defects**

Other types of defects including rail head defects, web defects, and joint-hole defects, should be considered when evaluating the reliability index. The structural reliability

theory can be performed both at single failure mode and at multiple failure modes. When implementing the analysis with respect to the multiple failure modes, rail defects are modeled as a series.

- **Numerical approach for calculating of the LCC**

Each expected cost to evaluate the LCC is drawn from an analytical approach, specifically an approximation method based on the least squares estimation. However, a numerical approach, such as the Morkov Chain Monte Carlo Simulation should be attempted to raise a precision of the evaluation of the expected reliability index.

- **Optimization for inspection intervals**

Rail defects tend to grow slowly and steadily at first, then the growth rate increases exponentially as the defects becomes larger. Therefore, non-uniform interval inspection may reduce the risk. Associated with this fact, variable interval inspection policy may also reduce the optimal number of inspections and the LCC.

- **Updating crack size information**

The LEFM analysis and the FORM analysis incorporate information of crack size with the results of NDT. In addition to the approach, updating the data should be done. This is because that whether any crack is detected or not, each inspection provides additional information about the probability distribution of the crack size. Thus, mathematical updating models, such as Bayesian approach, must be available to revise the information.

Appendix A

Equivalent Normal Variables

A.1 Rosenblatt Transformation

Hasofer-Lind reliability index can be exactly related to the failure probability, if all the variables are statistically independent and normally distributed and the limit state surface is linear. If not all the variables are normally distributed, as is common in engineering problems, it is necessary to transform the non-normal variables into equivalent normal variables.

In the section 3.2, probabilities involving non-normal distributions are calculated using equivalent normal distributions. In effect, this involves the transformation of a general set of correlated random variables into an equivalent set of independent Gaussian variates. A general transformation for this purpose is the Rosenblatt transformation (Rosenblatt 1952).

Suppose a set of n random variables $\underline{X} = (X_1, X_2, ..., X_n)$ with a joint Cumulative

Distribution Function (CDF) $F_{\underline{X}}(\underline{x})$. A set of statistically independent standard normal

variates, $\underline{U} = (U_1, U_2, ..., U_n)$ can be obtained from the following equations.

$$\Phi(u_1) = F_1(x_1)$$
$$\Phi(u_2) = F_2(x_2|x_1)$$
$$\Phi(u_3) = F_3(x_3|x_1, x_2) \qquad \text{(A.1)}$$
$$\vdots \qquad \vdots$$
$$\Phi(u_n) = F_n(x_n|x_1, x_2, ..., x_{n-1})$$

where, $\Phi(\bullet)$ is the CDF of standard normal variates. Inverting the above equations

successively, the desired normal variates $\underline{U}$ are obtained as follows.

$$u_1 = \Phi^{-1}[F_1(x_1)]$$
$$u_2 = \Phi^{-1}[F_2(x_2|x_1)]$$
$$u_3 = \Phi^{-1}[F_3(x_3|x_1, x_2)] \qquad \text{(A.2)}$$
$$\vdots \qquad \vdots$$
$$u_n = \Phi^{-1}[F_n(x_n|x_1, x_2, ..., x_{n-1})]$$

where, $\Phi^{-1}(\bullet)$ is the inverse function of the CDF of standard normal variates. The

equation (A.2) constitutes the Rosenblatt transformation.

The conditional CDFs in the equation (A.2) can be obtained from the joint PDFs

as follows.

Since

$$f(x_i|x_1, x_2, ...x_{i-1}) = \frac{f(x_1, x_2, ...x_i)}{f(x_1, x_2, ...x_{i-1})} \qquad \text{(A.3)}$$

the required CDF can be obtained as

$$F(x_i|x_1, x_2, ...x_{i-1}) = \frac{\int_{-\infty}^{x_i} f(\xi_1, \xi_2, ...\xi_{i-1})d\xi_i}{f(x_1, x_2, ...x_{i-1})} \qquad \text{(A.4)}$$

It is obvious that Rosenblatt transformation is available only when the joint CDF of all random variables is available.

A.2 Two-Parameter Equivalent Transformation

Because a normal random variable can be described uniquely by two parameters, any two conditions can be used for the transformation from non-normal variables into normal variables. Rackwitz and Fiessler (1978) estimate the parameters of the equivalent normal distribution, $\mu_{X_i}^N$ and $\sigma_{X_i}^N$ by imposing two conditions. The CDFs and PDFs of the actual variables and equivalent normal variables should be equal at the checking point $(x_1, x_2, ..., x_3)$ on the failure surface. Considering each statistically independent non-normal variable individually and equating its CDF with an equivalent normal variable at the checking point result in

$$F_{X_i}(x_i) = \Phi\left(\frac{x_i - \mu_{X_i}^N}{\sigma_{X_i}^N}\right) \tag{A.5}$$

where, $F_{X_i}(x_i)$ is the CDF of the original non-normal variable, and $\mu_{X_i}^N$ and $\sigma_{X_i}^N$ are the mean and standard deviation of the equivalent normal variable at the checking point. The equation (A.5) yields by Rosenblatt transformation

$$\frac{x_i - \mu_{X_i}^N}{\sigma_{X_i}^N} = \Phi^{-1}\left[F_{X_i}(x_i)\right]$$

$$\therefore \mu_{X_i}^N = x_i - \sigma_{X_i}^N \cdot \Phi^{-1}\left[F_{X_i}(x_i)\right] \tag{A.6}$$

Equating the PDFs of the original non-normal variable and the equivalent normal variable

at the checking point by differentiating the equation (A.5) results in

$$f_{X_i}(x_i) = \frac{1}{\sigma_{X_i}^N} \phi\left(\frac{x_i - \mu_{X_i}^N}{\sigma_{X_i}^N}\right) \qquad (A.7)$$

where, $\phi(\bullet)$ is the standard normal probability density function and f_{X_i} is the PDF of a original non-normal variable. Equation (A.7) yields

$$\sigma_{X_i}^N = \frac{\phi\{\Phi^{-1}[F_{X_i}(x_i)]\}}{f_{X_i}(x_i)} \qquad (A.8)$$

The mean value and the probability of excess of the equivalent normal variable are made equal to the median value and the probability of excess of the original non-normal variable, respectively, at the checking point. $\mu_{X_i}^N$ can be estimated as

$$\mu_{X_i}^N = F_{X_i}^{-1}(0.5) \qquad (A.9)$$

114

Appendix B

Reliability Index

B.1 Hasofer-Lind Reliability Index

The simplest way to explain the Hasofer-Lind reliability index is to examine the case of two independent random variables. Let R represent a random variable describing the strength or resistance of a system and let S represent a random variable describing the stress placed on the system. R and S are assumed to be statistically independent for simplicity. System failure occurs when the stress on the system exceeds the strength of the system: $\Omega = \{(r,s)|R < S\}$. Fig. B.1 shows the concepts of a Limit State Equation (LSE) and the associated failure/safe regions. The LSE can be expressed as follows:

$$G_1(R,S) = R - S$$
$$G_2(R,S) = \frac{R}{S} - 1 \tag{B.1}$$

According to the concept by Cornell (1969), the reliability index is defined as the value

115

where the mean value of the LSE is divided by the standard deviation of the LSE. Hence,

$$\beta = \frac{\mu_G}{\sigma_G} \tag{B.2}$$

where, μ_G and σ_G are the mean value and standard deviation of the LSE, respectively.

Therefore, the reliability index of equation (B.1) is:

$$\beta_1 = \frac{\mu_R - \mu_S}{\sqrt{\sigma_R^2 + \sigma_S^2}}$$

$$\beta_2 = \frac{\dfrac{\mu_R}{\mu_S} - 1}{\sqrt{\dfrac{\sigma_R^2}{\mu_R^2} + \dfrac{\mu_R^2}{\mu_S^4}\sigma_S^2}} = \frac{\mu_R \mu_S (\mu_R - \mu_S)}{\sqrt{\mu_R^4 \sigma_S^2 + \mu_S^4 \sigma_R^2}} \tag{B.3}$$

β_1 and β_2 are not identical, despite of the fact that each of the reliability indexes should give identical results. This indicates "the problem of invariance."

Hasofer and Lind (1974) suggest the method to overcome the problem of invariance by defining the reliability index as the minimum distance from origin to the LSE. They also introduce the reduced variates for normalization as follows:

$$R' = \frac{R - \mu_R}{\sigma_R}$$

$$S' = \frac{S - \mu_S}{\sigma_S} \tag{B.4}$$

The new LSE is defined in terms of reduced variates as follows:

$$G_1(R', S') = (\mu_R + \sigma_R R') - (\mu_S + \sigma_S S') = 0$$
$$\therefore \mu_R + \sigma_R R' = \mu_S + \sigma_S S'$$

$$\tag{B.5}$$

$$G_2(R', S') = \frac{\mu_R + \sigma_R R'}{\mu_S + \sigma_S S'} - 1 = 0$$
$$\therefore \mu_R + \sigma_R R' = \mu_S + \sigma_S S'$$

116

Graphically, the new LSE appears in Fig. B.2. Such a problem of invariance is circumvented as long as the reliability index is calculated by the minimum distance from origin to the new LSE in reduced coordinate, because each LSE of G_1 and G_2 is identical as shown above. Equating the new LSE:

$$S' = \frac{\sigma_R}{\sigma_S} R' + \frac{\mu_R - \mu_S}{\sigma_S} \qquad \text{(B.6)}$$

Then the Hasofer-Lind reliability index is:

$$\beta^2 = \frac{\sigma_R^2 (\mu_R - \mu_S)^2}{(\sigma_R^2 + \sigma_S^2)^2} + \frac{\sigma_S^2 (\mu_R - \mu_S)^2}{(\sigma_R^2 + \sigma_S^2)}$$

$$= \frac{\sigma_R^2 + \sigma_S^2}{(\sigma_R^2 + \sigma_S^2)^2} (\mu_R - \mu_S)^2 \qquad \text{(B.7)}$$

$$\therefore \beta = \frac{\mu_R - \mu_S}{\sqrt{\sigma_R^2 + \sigma_S^2}}$$
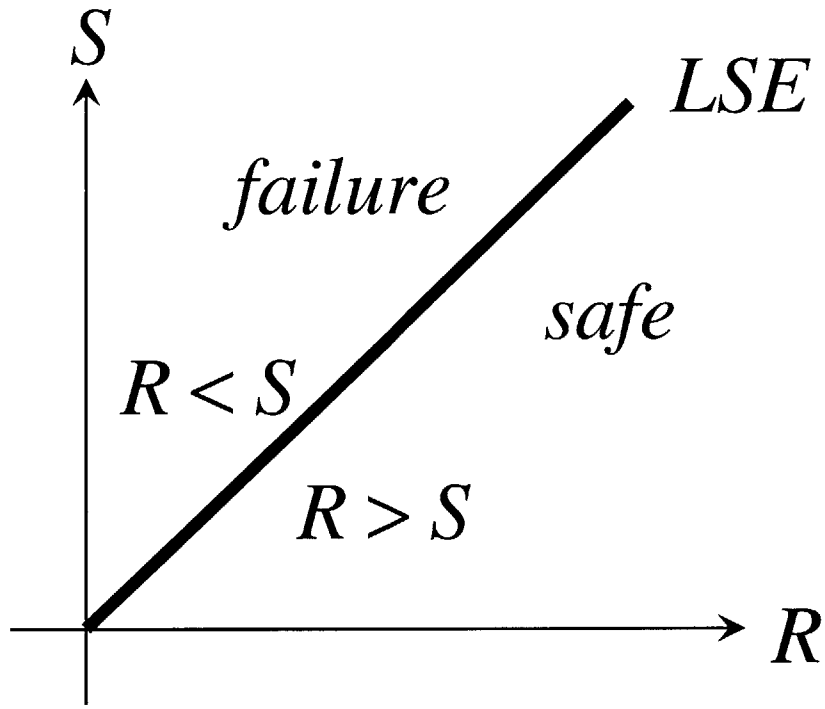
Fig. B.1 Limit State Equation in Two Random Variables
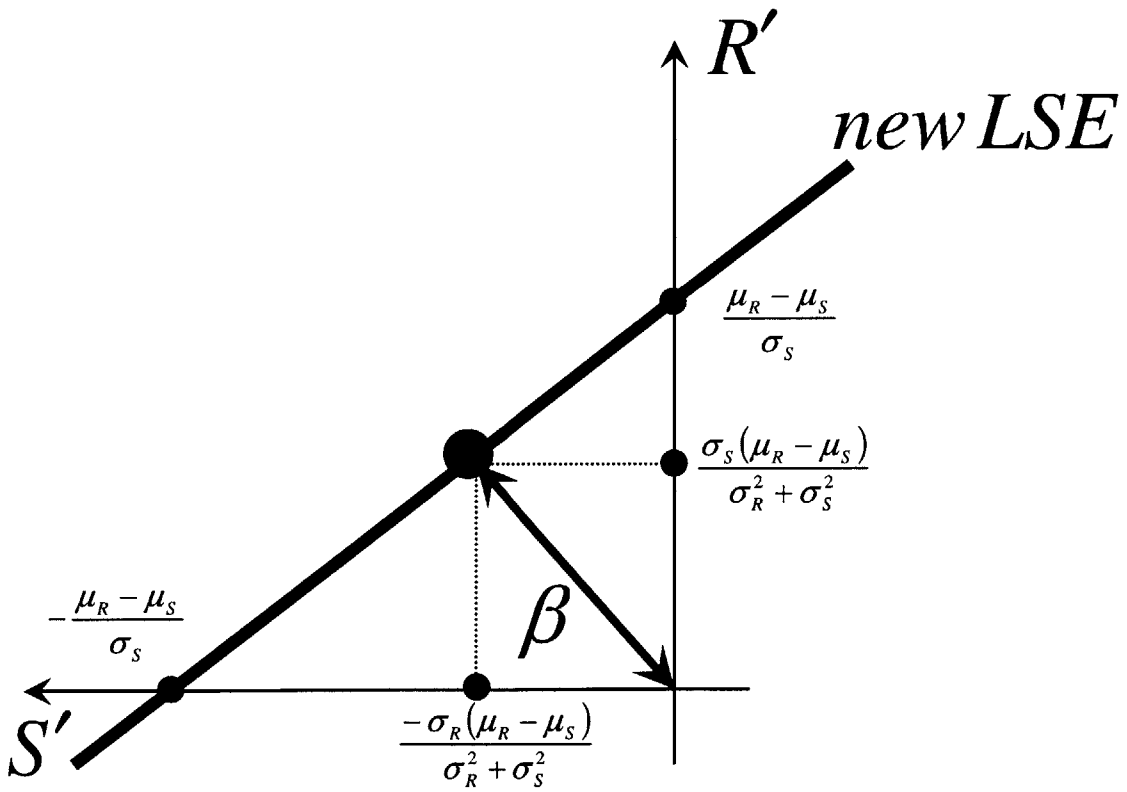

Fig. B.2 New Limit State Equation

118

B.2 Rackwitz-Fiessler Algorithm

As mentioned in the section B.1, it is necessary to search the minimum distance from the origin to the failure surface in reduced coordinate in order to evaluate the Hasofer-Lind reliability index. To solve the optimization problem expressed in the equation (3.25) in the section 3.3.1, many algorithms are presented. Newton-Raphson type recursive algorithm, also called Rackwitz-Fiessler algorithm (1978) is one of them.

The algorithm can be best explained with help of Fig.B.3 and B.4 in case of two independent random variables. First, consider the linear LSE shown in Fig.B.3. Since the limit sate is not available in a closed form, the starting point $\underline{x}_0$ may not be on the LSE $g(\underline{x}) = 0$, but on a parallel line $g(\underline{x}) = k$. Hence, the optimization algorithm has to start from point $\underline{x}_0$ which may not be on the LSE and converge to the minimum distance point $\underline{x}^*$ on the LSE. The linear LSE can be expressed as

$$g(\underline{x}) = b + \underline{a}^T \underline{x} \qquad (B.8)$$

where, $\underline{a}^T$ is the transpose of the gradient vector of the LSE. The magnitude of the vectors $\underline{x}_0, \underline{x}^*$ denote the distance from the origin to the starting point and the LSE, respectively. Using geometry, $\underline{x}^*$ can be expressed in terms of $\underline{x}_0$ as

$$\underline{x}^* = \frac{1}{|\underline{a}|} \left[\underline{a}^T \underline{x}_0 - g(\underline{x}_0) \right] \{\underline{a}\} \qquad (B.9)$$

Since the LSE is linear in this case, its gradient is constant. Hence, the distance to the LSE from the origin can be obtained in one step.

Next, equation (B.9) can be generalized for a non-linear LSE as shown Fig. B.4 as

$$\underline{x}_{k+1} = \frac{1}{\left|\nabla g(\underline{x}_k)\right|^2}\left[\nabla g(\underline{x}_k)^T \cdot g(\underline{x}_k) - g(\underline{x}_k)\right]\nabla g(\underline{x}_k) \qquad \text{(B.10)}$$

where, $\nabla g(\underline{x}_k)$ is the gradient vector of the LSE at $\underline{x}_k$, kth iteration point. Note that k refers to the iteration number. Since the LSE is not linear, the gradient is not constant but varies from one point to another point. Therefore, instead of one-step solution in case of linear LSE, the point of the minimum distance has to be searched through recursive formula given by equation (B.10). The LSE can be approximated by the tangent, first-order approximation at each iteration point. The LSE is linearized with $g(\underline{x}_k)$ and $\nabla g(\underline{x}_k)$ corresponding to $g(\underline{x}_0)$ and $\underline{a}$, respectively in the equation (B.9). The next iteration point is computed in the same way as in the case of the linear LSE. If the LSE is linear, $\underline{x}_{k+1}$ is identical to $\underline{x}_k$. However, its value and the gradient at $\underline{x}_{k+1}$ are different from those at $\underline{x}_k$. Therefore, it is again linearized at $\underline{x}_{k+1}$ and another iteration point $\underline{x}_{k+2}$ is computed. This algorithm is repeated until convergence meeting requirements of particular criteria.

In this First-Order Reliability Method (FORM) approach, the distance from the origin to the failure surface in the reduced coordinate is calculated by using first-order approximation at the each iteration point. When the LSE is not linear, the curvature of the LSE is not considered. Second-Order Reliability Method (SORM) and First-Order Third Moment (FOTM) (Zhao and Ang 2003) have been recently developed to improve precision of evaluation of the reliability index instead of FORM.
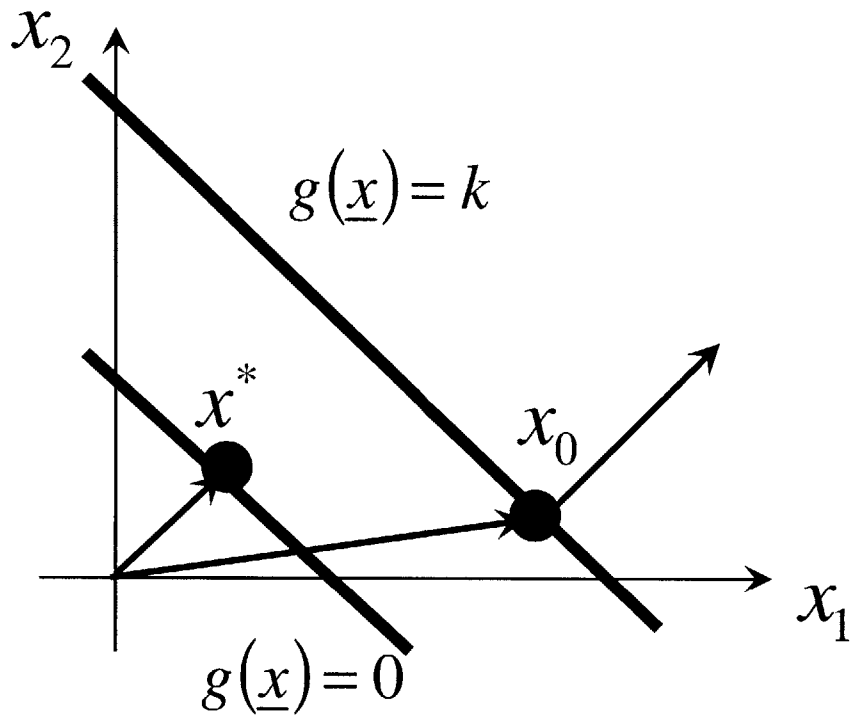
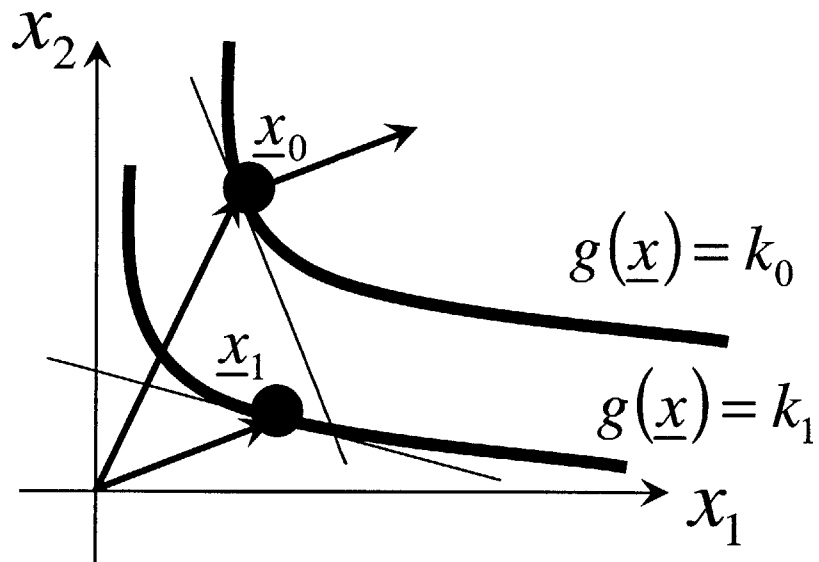**Fig. B.3 Searching Algorithm for a Linear LSE**

Fig. B.4 Searching Algorithm for a Non-Linear LSE

121

Bibliography

- Abraham M. Hasofer and Niels C. Lind (1974), "Exact and Invariant Second-Moment Code Format," Journal of Engineering Mechanics, ASCE, Vol.100, No.1, pp. 111-121.

- Achintya Haldar and Sankaran Mahadevan (2000), "Probability, Reliability and Statistical Methods in Engineering Design," John and Wiley & Sons, Inc.

- Alfredo H-S. Ang and Wilson H. Tang (1975), "Probability Concepts in Engineering Planning and Design Volume1," John and Wiley & Sons, Inc.

- Alfredo H-S. Ang and Wilson H. Tang (1984), "Probability Concepts in Engineering Planning and Design Volume2," John and Wiley & Sons, Inc.

- Allen C. Estes (1997), "A System Reliability Approach to the Lifetime Optimization of Inspection and Repair of Highway Bridges," Ph.D. Thesis, Department of Civil, Environmental and Architectural Engineering, University of Colorado, Boulder.

- Allen C. Estes and Dan M. Frangopol (2001), "Minimum Expected Cost-Oriented Optimal Maintenance Planning for Deteriorating Structures: Application to Concrete Bridge Decks," Reliability Engineering & System Safety, Vol.73, pp. 281-291.

- Cornell C. A. (1969), "A Probability-Based Structural Code," Journal of the American Concrete Institute, ACI, Vol.66, No.12, pp. 974-985.

- Dan M. Frangopol, Kai-Yung Lin, and Allen C. Estes (1997), "Life-Cycle Cost Design of Deteriorating Structures," Journal of Structural Engineering, ASCE, Vol.123, No.10, pp. 1390-1401.

- David Y. Jeong (2003), "Correlations between Rail Defect Growth Data and Engineering Analyses, Part1: Laboratory Tests," UIC/WEC Joint Research Project on Rail Defect Management, U.S. Department of Transportation, Research and Special Programs Administration, Volpe National Transportation Systems Center. *http://www.volpe.dot.gov/sdd/pubs-integrity.html*

- David Y. Jeong (2003), "Correlations between Rail Defect Growth Data and Engineering Analyses, Part2: Field Tests," UIC/WEC Joint Research Project on Rail Defect Management, U.S. Department of Transportation, Research and Special Programs Administration, Volpe National Transportation Systems Center. *http://www.volpe.dot.gov/sdd/pubs-integrity.html*

- David Y. Jeong (2003), "Analytical Modeling Rail Defects and its Applications to Rail Defect Management," UIC/WEC Joint Research Project on Rail Defect Management, U.S. Department of Transportation, Research and Special Programs Administration, Volpe National Transportation Systems Center. *http://www.volpe.dot.gov/sdd/pubs-integrity.html*

- Department of Transportation (2002), "Life-Cycle Cost Analysis Primer," *http://www.fhwa.dot.gov/infrastructure/asstmgmt/lcca.htm*

- Feng-Yeu Shyr (1993), "Combining Laboratory and Field Data in Rail Fatigue Analysis," Ph.D. Thesis, Department of Civil Engineering, Massachusetts Institute Technology.

- Eiji Yazawa (2000), "Kido to Syaryo no Sogo Sayo (2)," Nihon Tetsudo Shisetu Kyokai, Tetsudo Shisetsu Kyokaishi, April, pp. 282-285. (in Japanese)

- Henrik O. Madsen (1985), "Random Fatigue Crack Growth and Inspection," the proceedings of ICOSSAR'85, Vol.1, pp. 475-484.

- Henrik O. Madsen, J.D. Sorensen, and R. Olesen (1989), "Optimal Inspection Planning for Fatigue Damage of Offshore Structures," the proceedings ICOSSAR'89, pp. 2099-2106.

- Kenji Kashiwaya and Makoto Ishida (2003), "Prediction Model of Growth Rate of Rail Transverse Crack," the proceedings of Rail Mechanics, pp. 79-84. (in Japanese)

- L.P. Pook (2000), "Linear Elastic Fracture Mechanics for Engineers: Theory and Applications," WIT Press.

- P. Paris and F. Erdogan (1963), "A Critical Analysis of Crack Propagation Law," Journal of Basic Engineering, ASME, Vol.85, No.4, pp. 528-534.

- Qian Ma (1997), "Condition-Based Maintenance Applied to Rail Freight Car Components –The Case of Rail Car Trucks, Master Thesis, Department of Civil and Environmental Engineering, Massachusetts Institute Technology.

- Rackwitz R. and Fiessler B. (1978), "Structural Reliability under Combined Random Load Sequences," Computers and Structures, Vol.9, No. 5, pp. 489-494.

- Rosenblatt M. (1952), "Remarks on a Multivariate Transformation," Annals of Mathematical Statistics, Vol.23, No.3, pp. 470-472.

- Ruohua Zheng and Bruce R. Ellingwood (1998) "Pole of Non-Destructive Evaluation in Time-Dependant Reliability Analysis," Structural Safety, Vol.20, No. 4, pp. 325-339.

- Shooman M.L. (1968), "Probabilistic Reliability: an Engineering Approach," McGraw-Hill Book Co.

- Steven C. Lovejoy (2003), "Determining Appropriate Fatigue Inspection Intervals for Steel Bridge Members," Journal of Structural Engineering, ASCE, Vol.8, No.2, pp. 66-72.

- Thoft-Christensen P. and J.D. Sorensen (1987), "Optimal Strategies for Inspection and Repair of Structural Systems," Civil Engineering Systems, Vol.4, pp. 94-100.

- Toula Onoufriou (1999), "Reliability Based Inspection Planning of Offshore Structures," Marine Structures, Vol.12, pp. 521-539.

- Yan-Gang Zhao and Alfredo H-S. Ang (2003), "System Reliability Assessment by Mehod of Moments," Journal of Structural Engineering, ASCE, Vol.129, No.10, pp. 1341-1349.

- Yasuhiro Mori and Bruce R. Ellingwood (1984), "Maintaining Reliability of Concrete Structures," Journal of Structural Engineering, ASCE, Vol.120, No.3, pp. 824-845.

- Y. Garbatov and C. Guedes Soares (2001), "Cost and Reliability Based Strategy for Fatigue Maintenance Planning of Floating Structures," Reliability Engineering & System Safety, Vol.73, pp. 293-301.

- Yoshihiko Sato (1997), "Shin Kido Rikigaku," Tetsudo Gengyo-Sya. (in Japanese)

- Zhengwei Zhao, Achintya Haldar, and Florence L. Breen Jr. (1994), "Fatigue-Reliability Evaluation of Steel Bridges," Journal of Structural Engineering, ASCE, Vol.120, No.5, pp. 1608-1623.

- Zhengwei Zhao, Achintya Haldar, and Florence L. Breen Jr. (1994), "Fatigue-Reliability Updating through Inspections of Steel Bridges," Journal of Structural Engineering, ASCE, Vol.120, No.5, pp. 1624-1642.

H136 – 1